# Pentamethylcyclopentadienylrhodaborane Chemistry. Part 2.[1] The Reaction of [6-($\eta^5$-$C_5Me_5$)-*nido*-6-$RhB_9H_{13}$] with Dimethylphenylphosphine, and the Characterization of [5-($\eta^5$-$C_5Me_5$)-*nido*-5-$RhB_9H_{11}$-7-($PMe_2Ph$)], [2-($\eta^5$-$C_5Me_5$)-*closo*-2-$RhB_9H_7$-3,10-$(PMe_2Ph)_2$],* and [2-($\eta^5$-$C_5Me_5$)-*nido*-2-$RhB_8H_{10}$-5-($PMe_2Ph$)] by *X*-Ray Diffraction Analysis and Nuclear Magnetic Resonance Spectroscopy

**Xavier L. R. Fontaine, Hayat Fowkes, Norman N. Greenwood, John D. Kennedy, and Mark Thornton-Pett**
*Department of Inorganic and Structural Chemistry, University of Leeds, Leeds LS2 9JT*

Reaction of [6-($\eta^5$-$C_5Me_5$)-*nido*-6-$RhB_9H_{13}$] (**1**) with an excess of $PMe_2Ph$ in $CH_2Cl_2$ solution at room temperature yields three air-stable compounds: red-orange [5-($\eta^5$-$C_5Me_5$)-*nido*-5-$RhB_9H_{11}$-7-($PMe_2Ph$)] (**2**; 35%), yellow [2-($\eta^5$-$C_5Me_5$)-*closo*-2-$RhB_9H_7$-3,10-$(PMe_2Ph)_2$] (**3**; 25%), and orange [2-($\eta^5$-$C_5Me_5$)-*nido*-2-$RhB_8H_{10}$-5-($PMe_2Ph$)] (**4**; *ca.* 7%). Crystals of (**2**) are triclinic, space group $P\bar{1}$, with $a$ = 940.9(2), $b$ = 875.2(2), $c$ = 1 561.4(2) pm, $\alpha$ = 99.06(2), $\beta$ = 103.45(1), $\gamma$ = 91.57(2)°, and $Z$ = 2. Crystals of (**3**) are monoclinic, space group $P2_1/a$, with $a$ = 1 406.4(3), $b$ = 1 231.7(3), $c$ = 1 812.3(3) pm, $\beta$ = 94.01(1)°, and $Z$ = 4. These compounds, and compound (**4**), were also characterized by n.m.r. spectroscopy. Structural and bonding considerations are discussed and some mechanistic implications are briefly considered.

In Part 1 of this series we reported the quantitative reaction of [{Rh($\eta^5$-$C_5Me_5$)$Cl_2$}$_2$] with *arachno*-$[B_9H_{14}]^-$ to give the ten-vertex *nido*-6-metalladecaborane [6-($\eta^5$-$C_5Me_5$)-6-$RhB_9H_{13}$] (**1**).[1] The ready synthesis of this metallaborane in high yield from easily prepared starting materials facilitates the further examination of its chemistry, and here we report its reaction in solution with the tertiary phosphine $PMe_2Ph$ under mild conditions. Some preliminary aspects of this work have been presented elsewhere.[2-4] Numbering systems for the cluster types encountered in this work are given in structures (**I**) (*nido* ten-vertex), (**II**) (*closo* ten-vertex), and (**III**) (*nido* nine-vertex). Note that interconversions among these structures will generally change the numbering of a particular atom.

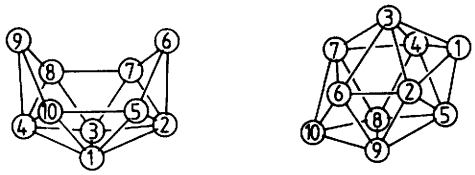


(I) (II) (III)

## Results and Discussion

(a) *Reaction of* [6-($\eta^5$-$C_5Me_5$)-*nido*-6-$RhB_9H_{13}$] (**1**) *with* $PMe_2Ph$.—Reaction of (**1**) with an excess of $PMe_2Ph$ in dichloromethane solution for 30 min at room temperature, followed by chromatographic separation of the products, yielded three brightly coloured rhodaborane products, compounds (**2**), (**3**), and (**4**) (Scheme 1); under these conditions all the rhodaborane starting material (**1**) was consumed. A number of minor products ($\leqslant$ *ca.* 2% yield of each), which were either unstable or obtained in yields insufficiently large for further investigation, were also formed.

Red-orange (**2**) and yellow (**3**) were both air stable in the solid state, and reasonably robust in solution; they were identified by single-crystal *X*-ray diffraction analysis as [5-($\eta^5$-$C_5Me_5$)-*nido*-5-$RhB_9H_{11}$-7-($PMe_2Ph$)] and [2-($\eta^5$-$C_5Me_5$)-*closo*-2-$RhB_9H_7$-3,10-$(PMe_2Ph)_2$] respectively. Isolated yields (*ca.* 1 mmol scale reaction) were 35 and 25% respectively, and n.m.r. spectroscopy confirmed the identities of the bulk samples. Orange (**4**) was isolable in lower, more variable, yield (2—7%), and although stable for reasonable periods (weeks) in the pure solid state was less stable in solution than (**2**) and (**3**). This solution instability has so far precluded the growing of crystals suitable for single-crystal *X*-ray diffraction work, but the identity of (**4**) as [2-($\eta^5$-$C_5Me_5$)-*nido*-2-$RhB_8H_{10}$-5-($PMe_2Ph$)] [numbering as in (**III**)] readily follows from n.m.r. spectroscopy.

The reaction between equimolar quantities of compound (**1**) and $PMe_2Ph$ in dichloromethane solution was monitored by integrated n.m.r. spectroscopy; after 2 h reaction time the molar proportions of compounds (**1**)—(**4**) were *ca.* 13:3:7:1 respectively, and other minor components of molarity similar to or less than that of (**4**) were also apparent. One of these was readily identified by n.m.r. as $BH_3(PMe_2Ph)$ [molar proportion *ca.* 1 with respect to compound (**1**) taken as 13]; some of the others had deshielded $^{11}B$ metallaboranyl features which suggested that they may be isomers or close structural analogues of compounds (**2**)—(**4**).

(b) *Characterization of* [5-($\eta^5$-$C_5Me_5$)-*nido*-5-$RhB_9H_{11}$-7-($PMe_2Ph$)] (**2**).—The molecular structure of (**2**) was determined by single-crystal *X*-ray diffraction analysis (Figure 1, and Tables 1 and 2). All cluster hydrogen atoms were readily located

* *nido*-7-(Dimethylphenylphosphine)-5-($\eta^5$-pentamethylcyclopentadienyl)-5-rhodadecaborane and *closo*-3,10-bis(dimethylphenylphosphine)-2-($\eta^5$-pentamethylcyclopentadienyl)-2-rhodadecaborane respectively.

*Supplementary data available:* see Instructions for Authors, *J. Chem. Soc., Dalton Trans.*, 1987, Issue 1, pp. xvii—xx.

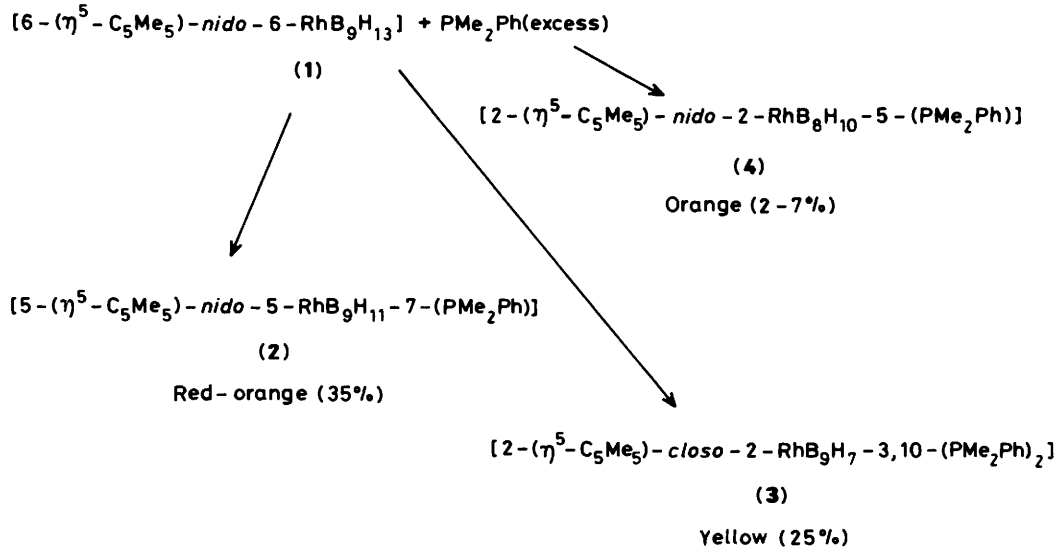


**Scheme 1.**

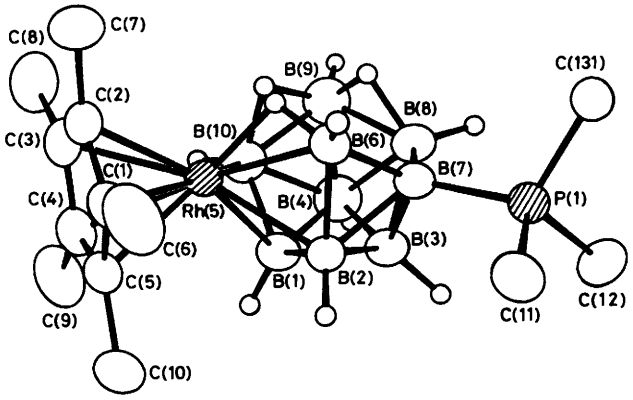


**Figure 1.** ORTEP drawing of the molecular structure of [5-(η⁵-$C_5Me_5$)-*nido*-5-$RhB_9H_{11}$-7-($PMe_2Ph$)] (**2**) with methyl and phenyl hydrogen atoms and P-phenyl carbon atoms other than the *ipso* one omitted for clarity

in Fourier difference maps and freely refined to reasonable positions. The compound is seen to have the open-boat ten-vertex cluster configuration of *nido*-$B_{10}H_{14}$ but with the B(5) position subrogated by the rhodium atom. The bridging hydrogen atom positions, together with other general characteristics including n.m.r. properties (see Table 3 and Figure 2) establish the structure as *nido* rather than *arachno*. There is an *exo*-($PMe_2Ph$) ligand pendant to the cluster at the 7 position, the rhodium atom retains the η⁵-$C_5Me_5$ ligand of the starting halide, and so the compound is formulated as [5-(η⁵-$C_5Me_5$)-*nido*-5-$RhB_9H_{11}$-7-($PMe_2Ph$)].

Although there are as yet limited metallaborane data for detailed comparison (refs. 1, 5—9, and Table 4), the rhodium–boron distances of 216.8(6)—226.2(6) pm are towards the centre of the established range of *ca.* 205—230 pm. The B(7)–B(8) distance, adjacent to the phosphine ligand, is shorter at 179.1(7) pm than in other *nido*-decaboranyl clusters (*e.g.* 197 pm in $B_{10}H_{14}$ itself) although this may be a function of the increased electron density on B(7) arising from the phosphine donation[10] since in a related 5-ruthenaborane [(η⁶-$C_6Me_6$)-$RuB_9H_{12}$(OMe)][10a] which does not have a phosphine in this position the B(5)–B(10) distance is 196.2(9) pm. Likewise in [6,6,6-($PPh_3$)$_2$H-*nido*-6-$RuB_9H_{12}$-7-($PPh_3$)] there is no similar

**Table 1.** Selected interatomic distances (pm) for [5-(η⁵-$C_5Me_5$)-5-$RhB_9H_{11}$-7-($PMe_2Ph$)] (**2**) with estimated standard deviations (e.s.d.s) in parentheses

| | | | |
|---|---|---|---|
| *(i)* From the rhodium atom | | | |
| Rh(5)–C(1) | 221.4(5) | Rh(5)–B(1) | 220.5(6) |
| Rh(5)–C(2) | 222.1(5) | Rh(5)–B(2) | 220.4(5) |
| Rh(5)–C(3) | 223.4(5) | Rh(5)–B(6) | 216.8(6) |
| Rh(5)–C(4) | 220.3(5) | Rh(5)–B(10) | 226.2(6) |
| Rh(5)–C(5) | 219.3(5) | Rh(5)–H(5,6) | 164(6) |
| *(ii)* Boron–boron | | | |
| B(1)–B(2) | 178.0(7) | B(2)–B(3) | 174.8(7) |
| B(1)–B(3) | 177.3(7) | | |
| B(1)–B(4) | 179.6(8) | B(3)–B(4) | 177.4(8) |
| B(1)–B(10) | 177.3(8) | B(3)–B(8) | 181.9(7) |
| B(2)–B(6) | 181.9(7) | B(4)–B(9) | 171.2(8) |
| B(3)–B(7) | 172.5(7) | | |
| B(4)–B(8) | 182.9(8) | B(4)–B(10) | 176.8(8) |
| B(7)–B(8) | 179.1(7) | | |
| B(9)–B(10) | 179.2(8) | B(8)–B(9) | 183.2(8) |
| *(iii)* Boron–hydrogen | | | |
| B(1)–H(1) | 106(3) | B(3)–H(3) | 123(4) |
| B(2)–H(2) | 110(3) | B(4)–H(4) | 120(4) |
| B(6)–H(6) | 101(4) | B(9)–H(9) | 113(4) |
| B(10)–H(10) | 104(5) | B(8)–H(8) | 118(3) |
| B(6)–H(5,6) | 115(6) | | |
| B(8)–H(8,9) | 138(4) | B(10)–H(9,10) | 133(4) |
| B(9)–H(8,9) | 118(4) | B(9)–H(9,10) | 123(4) |
| *(iv)* Others | | | |
| B(7)–P(1) | 190.7(6) | P(1)–C(11) | 180.7(5) |
| P(1)–C(12) | 180.9(5) | P(1)–C(131) | 180.5(4) |
| C–C(cyclic) | 141.0(6)—142.9(6) | C–C(terminal) | 149.9(6)—151.3(7) |

shortening of B(5)–B(10) at 201.1(22) pm.[11] This latter compound retains the μ(6,7) bridging hydride though, whereas in (**2**) B(6)–B(7) is unbridged and is short at 165.7(7) pm. This shortening is as generally observed[9,12] upon deprotonation of a B–H–B bridging system [as has effectively occurred in the comparison of compound (**2**) with the ruthenaborane] and implies substantial two-electron two-centre character in the

**Table 2.** Selected angles between interatomic vectors (°) for [5-($\eta^5$-$C_5Me_5$)-5-$RhB_9H_{11}$-7-($PMe_2Ph$)] (**2**) with e.s.d.s in parentheses

| | | | |
|---|---|---|---|
| (*i*) Boron–rhodium–boron | | | |
| B(1)–Rh(5)–B(2) | 47.6(1) | B(2)–Rh(5)–B(6) | 49.2(1) |
| B(1)–Rh(5)–B(6) | 87.0(2) | B(2)–Rh(5)–B(10) | 86.3(2) |
| B(1)–Rh(5)–B(10) | 46.7(1) | B(6)–Rh(5)–B(10) | 98.4(3) |
| (*ii*) Rhodium–boron–boron | | | |
| Rh(5)–B(1)–B(2) | 66.2(3) | Rh(5)–B(2)–B(1) | 66.2(3) |
| Rh(5)–B(1)–B(3) | 113.8(3) | Rh(5)–B(2)–B(3) | 115.0(3) |
| Rh(5)–B(1)–B(4) | 117.1(3) | Rh(5)–B(2)–B(6) | 64.4(3) |
| Rh(5)–B(1)–B(10) | 68.3(3) | Rh(5)–B(2)–B(7) | 107.8(3) |
| Rh(5)–B(6)–B(2) | 66.4(3) | Rh(5)–B(10)–B(4) | 115.5(3) |
| Rh(5)–B(6)–B(7) | 114.4(3) | Rh(5)–B(10)–B(9) | 117.7(3) |
| Rh(5)–B(10)–B(1) | 64.9(3) | | |
| (*iii*) Others | | | |
| B(6)–B(7)–B(8) | 115.1(4) | B(7)–B(8)–B(9) | 123.6(4) |
| B(8)–B(9)–B(10) | 104.1(4) | | |
| Rh(5)–H(5,6)–B(6) | 100(4) | | |
| B(8)–H(8,9)–B(9) | 91(3) | B(9)–H(9,10)–B(10) | 89(2) |
| P(1)–B(7)–B(2) | 119.2(3) | P(1)–B(7)–B(6) | 116.9(3) |
| P(1)–B(7)–B(3) | 116.1(3) | P(1)–B(7)–B(8) | 119.5(3) |

resulting interboron bond. Similar behaviour is exhibited by *nido*-5-iridadecaboranes and their 7-phosphine substituted analogues.[13]

In cluster terms the metallaborane unit in (**2**) is an analogue of *nido*-$[B_{10}H_{13}]^-$, in which the 7-positioned $BH^-$ adjacent to the deprotonated B(6)–B(7) link had been notionally replaced by the isoelectronic neutral fragment $B(PMe_2Ph)$, and in which the 5-positioned BH neutral moiety has been replaced by its isoelectronic and isolobal cluster subrogator $Rh(C_5Me_5)$. The rhodium centre contributes three orbitals and two electrons to the formal cluster-bonding scheme and electron count, which together with the $\eta^5$-$C_5Me_5$ ligand indicate that it can be regarded as a straightforward 'octahedral' six valence-orbital 18-electron $d^6$ rhodium(III) centre.

Compound (**2**) can also be regarded as having a two-decker sandwich character: the $\eta^5$-$C_5$ plane and the B(1)B(2)B(6)B(10) plane being nearly parallel (dihedral angle 3.0°), as similarly observed for [6-($\eta^5$-$C_5Me_5$)-*nido*-6-$RhB_9H_{13}$] (**1**),[1] [2-($\eta^5$-$C_5Me_5$)-*closo*-2-$RhB_9H_7$-3,10-$(PMe_2Ph)_2$] [(**3**), see below], and also for a variety of related cobalt species.[14,15] It is interesting that the five methyl groups on the cyclopentadienyl ring are distorted out of the $\eta^5$-$C_5$ plane, being bent *away* slightly from the metal atom (range of angular deviation from the $\eta^5$-$C_5$ plane 1.9—3.2°). This is again as observed for compounds (**1**) and (**3**), but contrasts to the behaviour observed for a variety of related metallaboranes and metallacarboranes of first-row transition elements such as iron and cobalt, in which the methyl groups are distorted out of the $\eta^5$-$C_5$ plane *towards* the metal atom.[16]

The n.m.r. properties (Table 3 and Figure 2) are consistent with the above molecular structure (confirming that the crystal was representative of the bulk sample), two-dimensional [$^{11}$B–$^{11}$B]-COSY[17–19] spectroscopy together with $^1$H-{$^{11}$B-(selective)}[20,21] spectroscopy permitting the assignment of the $^{11}$B and $^1$H resonances to cluster positions. Of interest are the extreme shifts of $^{11}$B(2) and $^{11}$B(6) to lower shielding {$\Delta\sigma$ (change in shielding) −40.4 and −53.8 p.p.m. respectively] compared to those[22,23] in the parent $B_{10}H_{14}$ molecule. These are positions adjacent (α) to the metal atom, but in this regard the shifts of $^{11}$B(1) and $^{11}$B(10) ($\Delta\sigma$ +6.1 and 0 p.p.m. respectively), also α to the metal atom, are relatively small, and

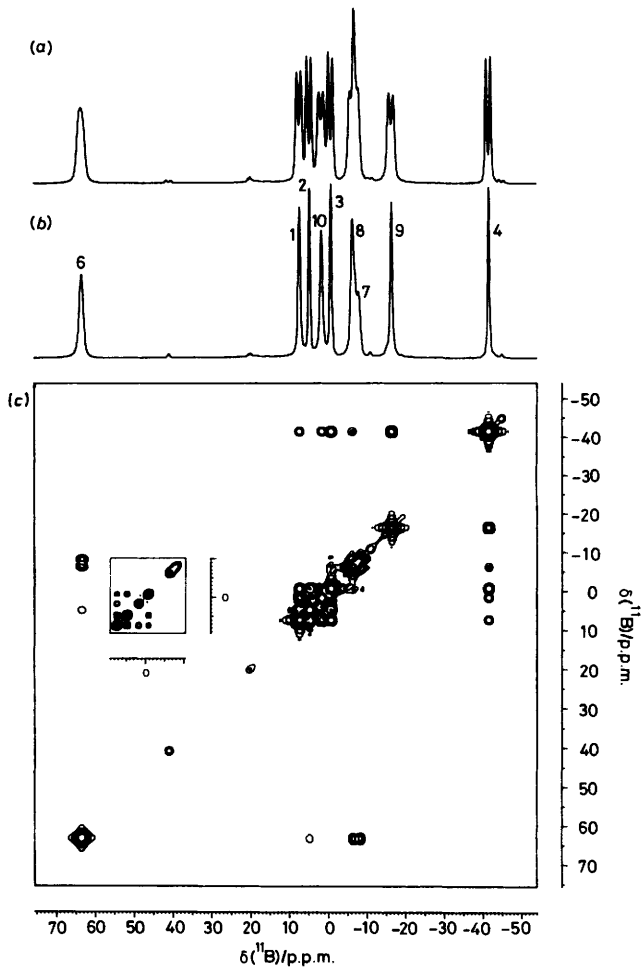


**Figure 2.** 128-MHz $^{11}$B n.m.r. spectra of [5-($\eta^5$-$C_5Me_5$)-*nido*-5-$RhB_9H_{11}$-7-($PMe_2Ph$)] (**2**) in $C_6D_5CD_3$ solution at +90 °C. (*a*) Straightforward $^{11}$B spectrum. (*b*) $^{11}$B Spectrum recorded under conditions of {$^1$H(broad-band noise)} decoupling. (*c*) [$^{11}$B-$^{11}$B]-COSY 90 contour plot, for which data were also gathered under conditions of {$^1$H(broad-band noise)} decoupling. The vignette shows the results, for the central crowded region [$\delta(^{11}H)$ *ca.* +10 to *ca.* −10 p.p.m.], of a COSY 45 experiment (same scale as the major diagram). This reduces the intensity in the diagonal and thus permits the better observation of any cross peaks between closely spaced resonances

the $^{11}$B(9) resonance ($\Delta\sigma$ +27.7 p.p.m.), now β to the metal atom, has a large positive shielding increment when compared to $B_{10}H_{14}$. The large perturbations, particularly the non-α one, contrast to the minor ones observed when the centres IrH-$(PPh_3)_2$, $Os(PMe_2Ph)_3$, $ReH(PMe_2Ph)_3$, and $WH_2(PMe_2Ph)_3$ subrogate the 6-BH position in $B_{10}H_{14}$,[24] which suggests that 5-BH subrogation by a metal centre produces a much greater perturbation of the *nido*-decaborane cluster electronic structure than does a 6-BH subrogation. It is however apparent that these observed shifts are also a function of metal character, since $Rh(\eta^5$-$C_5Me_5)$ at the 6 position also produces non-trivial shielding changes [$\Delta\sigma(\alpha)$ −20 to −25 p.p.m., $\Delta\sigma(\gamma)$ +15 p.p.m.].[1] These could arise from changes in electron density and/or symmetry, but also imply o.m.o.–u.m.o. (occupied, and unoccupied, molecular orbitals, respectively) excitations among molecular orbitals that involve *both* these $RhC_5$ and $RhB_9$ sub-clusters.

Cluster bonding asymmetry is also apparent from the observed [$^{11}$B–$^{11}$B]-COSY correlations [Table 3, Figure 2, and structure (**IV**)]. There are strong correlations between adjacent pairs of $^{11}$B nuclei in the 1, 2, 3, and 4 positions, and also

**Table 3.** Measured n.m.r. data for [5-($\eta^5$-$C_5Me_5$)-*nido*-$RhB_9H_{11}$-7-($PMe_2Ph$)] (**2**)

| Assignment[a] | $\delta(^{11}B)$/p.p.m.[b] $CDCl_3$ solution (294 K) | $\delta(^1H)$/p.p.m.[c] $CD_2Cl_2$ solution (294 K) | $^1J(^{11}B-^1H)$/Hz[d] $C_6D_5CD_3$ solution (363 K) | $\delta(^{11}B)$/p.p.m.[b] $C_6D_5CD_3$ solution (363 K) | Observed [$^{11}B-^{11}B$]-COSY correlations[e] $C_6D_5CD_3$ solution (363 K) |
|---|---|---|---|---|---|
| 1 | +6.0 | +2.38 | 158 | +7.3 | 2s 3s 4s 10s |
| 2 | +4.3 | +1.54 | 139 | +4.7 | 1s 3s 6w |
| 3 | −2.0 | +1.90 | 138 | −0.9 | 1s 2s 4s 7w 8w |
| 4 | −42.1 | −0.04 | 145 | −41.6 | 1s 3s 8s 9vs 10s |
| 5 | Rh position | $C_5Me_5$[f] | | Rh position | |
| 6 | +64.0 | +6.37 | *ca.* 140[g] | +63.3 | 2w 7s |
| 7 | −7.6[h] | $PMe_2Ph$[i] | *ca.* 150[j] | −7.5[h] | 3w 6s 8w |
| 8 | −7.0 | +1.76 | *ca.* 150[j] | −6.4 | 3w 4s 7w |
| 9 | −17.5 | +2.06 | 154 | −16.5 | 4vs |
| 10 | +0.6 | +3.01 | 145 | +1.6 | 1s 4s |
| 5,6 (bridge) | | −14.81[k] | | | |
| 8,9 (bridge) | | −3.33[l] | | | |
| 9,10 (bridge) | | −1.91[m] | | | |

[a] Assignments by $^1H$-{$^{11}B$} and two-dimensional [$^{11}B-^{11}B$]-COSY experiments. Numbering as in structure (**I**) and Figure 1. [b] ±0.5 p.p.m. to high frequency (low field) of $BF_3(OEt_2)$ in $CDCl_3$. [c] ±0.05 p.p.m. to high frequency (low field) of $SiMe_4$; $^1H$ resonances assigned to directly-bound B positions by $^1H$-{$^{11}B$(selective)} spectroscopy. [d] ± 5 Hz, measured from $^{11}B$ spectra with resolution enhancement to achieve baseline separation of doublet components. [e] s = Strong, w = weak, v = very; note that observed intensities depend on *both* $^1J(^{11}B-^{11}B)$ *and* $T_2^*$ ($^{11}B$) and therefore upon solution conditions. [f] $\delta(^1H)(C_5Me_5)$ + 1.81 p.p.m. Fine structure apparent in $^1H$-{$^{11}B$(broad-band noise)} spectrum, arising from couplings $^3J(^{103}Rh-^1H)$ 0.46 Hz and $^4J(^1H-^1H)$ *ca.* 0.6 Hz to $^1H$(5,6)(bridge) (see also footnote *k*). [g] Major splitting of *ca.* 140 Hz partially obscured by two other apparent splittings each of *ca.* 60 Hz. [h] $^1J(^{31}P-^{11}B)$(*exo*) *ca.* 120 Hz. [i] $\delta(^{31}P)$ *ca.* −2.0 p.p.m. to high frequency (low field) of 85% $H_3PO_4$; broad quartet; in $CDCl_3$ solution at 294 K; $^1H$ spectrum showed two independent P-methyl resonances [B(7) is a chiral centre] at $\delta(^1H)$ +1.89 and +1.79 p.p.m. [each with $^2J(^{31}P-C-^1H)$ *ca.* 11.5 Hz]. [j] Overlapping B(7) and B(8) resonances preclude more accurate estimation. [k] Selectively sharpened only by $\nu[^{11}B(6)]$ in $^1H$-{$^{11}B$(selective)} experiments; splitting of 36 Hz ascribed to $^1J(^{103}Rh-^1H)$, rather than to $^2J(^{31}P-B-^1H)$; also exhibits $^2J$ coupling to $^1H(6)$ of $\leqslant$ *ca.* 7 Hz and $^4J$ coupling to $^1H$(CMe) of *ca.* 0.6 Hz [established by $^1H$-{$^1H$(selective), $^{11}B$(broad-band noise)} experiments at 400 MHz], plus an additional splitting of 9 Hz from either $^1H(2)$ or $^{31}P$. [l] Strongly correlated with B(9) but only weakly with $^{11}B(8)$ in $^1H$-{$^{11}B$(selective)} experiments. [m] Strongly correlated with $^{11}B(9)$ but only weakly with $^{11}B(10)$ in $^1H$-{$^{11}B$(selective)} experiments.

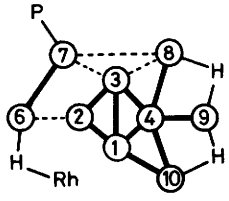


(IV)

between B(4) and B(9), all as observed in other *nido*-decaboranyl species.[17–19,23,25,26] In addition, $^{11}B(8)$–$^{11}B(9)$ and $^{11}B(9)$–$^{11}B(10)$ correlations were not observed, consistent with the weak interboron coupling associated with B–H–B bonds also observed in other *nido*-decaboranyl species.[17–19,23,25,26] In contrast to other *nido*-decaboranyl systems, however, the correlation $^{11}B(2)$–$^{11}B(6)$, adjacent to the metal centre, is weak, and conversely the unbridged $^{11}B(6)$–$^{11}B(7)$ correlation, now associated with a short interboron bond (see above and Table 1) is strong. Also, a possible (weak) $^{11}B(7)$–$^{11}B(8)$ correlation appeared to be present on some COSY plots, whereas it is usually not observed for the (generally longer) B(7)–B(8) and B(5)–B(10) linkages in *nido*-decaboranyl species. Furthermore, the observed strong $^{11}B(1)$–$^{11}B(10)$ correlation is not mirrored by a strong $^{11}B(3)$–$^{11}B(8)$ correlation on the other side of the molecule.

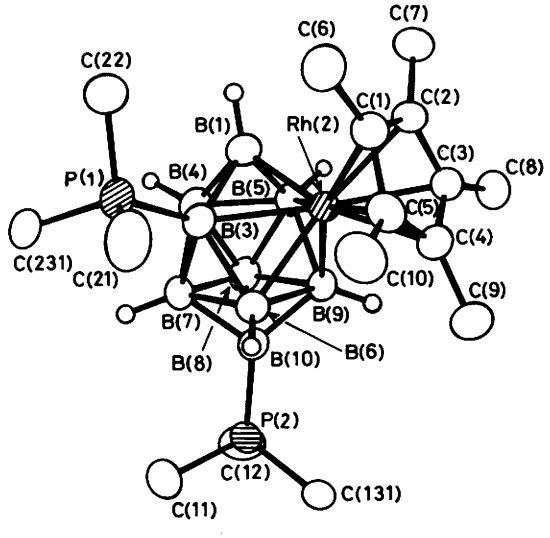


**Figure 3.** ORTEP drawing of the molecular structure of [2-($\eta^5$-$C_5Me_5$)-*closo*-2-$RhB_9H_7$-3,10-($PMe_2Ph)_2$] (**3**) with methyl and phenyl hydrogen atoms and P-phenyl carbon atoms other than the *ipso* ones omitted for clarity

(c) *Characterization of* [2-($\eta^5$-$C_5Me_5$)-*closo*-2-$RhB_9H_7$-3,10-($PMe_2Ph)_2$] (**3**).—The molecular structure of (**3**) was determined by single-crystal *X*-ray diffraction analysis (Figure 3 and Tables 4 and 5), all cluster hydrogen atoms being located. The basic metallaborane cluster geometry is seen to be based on the bicapped square antiprismatic cluster typified by *closo*-$[B_{10}H_{10}]^{2-}$, but with one of the 'tropical' 5-connected BH positions [nominally B(2)] subrogated by the isoelectronic and isolobal Rh($\eta^5$-$C_5Me_5$) moiety, and with two B–phosphine ligand substituents, one on an adjacent B(3) atom in the same tropical belt, and the other on the distant axial B(10) atom. Each of these two $B(PMe_2Ph)$ moieties is isolobal and isoelectronic in cluster terms with $BH^-$ and so the compound is a direct *closo*-$[B_{10}H_{10}]^{2-}$ analogue and thus formulated as

**Table 4.** Selected interatomic distances (pm) for [2-($\eta^5$-$C_5Me_5$)-2-$RhB_9H_7$-3,10-($PMe_2Ph$)$_2$] (**3**) with e.s.d.s in parentheses

| | | | |
|---|---|---|---|
| *(i)* To the rhodium atom | | | |
| Rh(2)–B(1) | 204.9(6) | | |
| Rh(2)–B(3) | 223.7(6) | Rh(2)–B(5) | 226.1(6) |
| Rh(2)–B(6) | 220.3(6) | Rh(2)–B(9) | 220.9(6) |
| Rh(2)–C(1) | 224.5(5) | | |
| Rh(2)–C(2) | 223.3(5) | Rh(2)–C(5) | 224.9(5) |
| Rh(2)–C(3) | 221.1(5) | Rh(2)–C(4) | 225.8(6) |
| *(ii)* Boron–boron | | | |
| B(1)–B(3) | 172.2(8) | B(1)–B(5) | 173.0(7) |
| B(1)–B(4) | 170.4(8) | | |
| B(3)–B(4) | 181.5(7) | B(5)–B(4) | 183.3(8) |
| B(3)–B(6) | 181.4(7) | B(5)–B(8) | 180.3(8) |
| B(3)–B(7) | 179.8(8) | B(5)–B(9) | 181.4(8) |
| B(4)–B(7) | 180.9(8) | B(4)–B(8) | 179.8(8) |
| B(6)–B(7) | 184.5(8) | B(9)–B(8) | 182.8(8) |
| B(6)–B(10) | 168.4(8) | B(9)–B(10) | 168.5(8) |
| B(6)–B(9) | 199.9(8) | | |
| B(7)–B(8) | 183.3(8) | | |
| B(7)–B(10) | 168.6(8) | B(8)–B(10) | 169.6(8) |
| *(iii)* Boron–hydrogen | | | |
| B(1)–H(1) | 107(3) | B(7)–H(7) | 107(3) |
| B(4)–H(4) | 116(3) | B(8)–H(8) | 119(4) |
| B(5)–H(5) | 118(3) | B(9)–H(9) | 105(4) |
| B(6)–H(6) | 113(4) | | |
| *(iv)* Others | | | |
| P(1)–B(3) | 189.8(6) | P(2)–B(10) | 186.8(6) |
| P(1)–C(11) | 179.1(6) | P(2)–C(21) | 179.7(6) |
| P(1)–C(12) | 181.0(6) | P(2)–C(22) | 181.0(6) |
| P(1)–C(131) | 179.5(4) | P(2)–C(231) | 179.3(4) |
| C–C(cyclic) | 141.2(6)—144.2(6) | C–C(terminal) | 149.6(6)—151.0(7) |

**Table 5.** Selected angles between interatomic vectors (°) for [2-($\eta^5$-$C_5Me_5$)-2-$RhB_9H_7$-3,10-($PMe_2Ph$)$_2$] (**3**) with e.s.d.s in parentheses

| | | | |
|---|---|---|---|
| *(i)* At the rhodium atom | | | |
| B(1)–Rh(2)–B(3) | 47.1(2) | B(1)–Rh(2)–B(5) | 47.0(2) |
| B(1)–Rh(2)–B(6) | 89.9(3) | B(1)–Rh(2)–B(9) | 89.1(3) |
| B(3)–Rh(2)–B(6) | 48.2(1) | B(5)–Rh(2)–B(9) | 47.9(1) |
| B(3)–Rh(2)–B(9) | 81.2(3) | B(5)–Rh(2)–B(6) | 82.1(3) |
| B(6)–Rh(2)–B(9) | 53.9(3) | | |
| *(ii)* Boron–boron–rhodium | | | |
| B(3)–B(1)–Rh(2) | 72.2(3) | B(5)–B(1)–Rh(2) | 73.0(3) |
| B(4)–B(1)–Rh(2) | 111.7(4) | | |
| B(1)–B(3)–Rh(2) | 60.7(3) | B(1)–B(5)–Rh(2) | 60.0(3) |
| B(4)–B(3)–Rh(2) | 99.8(3) | B(4)–B(5)–Rh(2) | 98.4(3) |
| B(6)–B(3)–Rh(2) | 64.9(3) | B(9)–B(5)–Rh(2) | 64.6(3) |
| B(7)–B(3)–Rh(2) | 112.3(3) | B(8)–B(5)–Rh(2) | 110.9(3) |
| B(3)–B(6)–Rh(2) | 66.9(3) | B(5)–B(9)–Rh(2) | 67.6(3) |
| B(7)–B(6)–Rh(2) | 111.9(3) | B(8)–B(9)–Rh(2) | 112.2(3) |
| B(9)–B(6)–Rh(2) | 63.2(3) | B(6)–B(9)–Rh(2) | 62.9(3) |
| B(10)–B(6)–Rh(2) | 115.6(4) | B(10)–B(9)–Rh(2) | 115.3(4) |
| *(iii)* Boron–boron–boron | | | |
| B(3)–B(1)–B(4) | 64.0(3) | B(5)–B(1)–B(4) | 64.5(4) |
| B(3)–B(1)–B(5) | 97.7(4) | | |
| B(6)–B(10)–B(7) | 66.4(3) | B(9)–B(10)–B(8) | 65.5(3) |
| B(6)–B(10)–B(8) | 103.7(4) | B(9)–B(10)–B(7) | 103.5(4) |
| B(6)–B(10)–B(9) | 72.8(4) | | |
| B(7)–B(10)–B(6) | 66.4(4) | | |
| For the 'tropical' boron atoms | | | |
| B–B–B(acute) | 56.8(3)—61.4(3) | B–B–B(obtuse) | 87.0(3)—116.4(4) |
| *(iv)* Phosphorus–boron–boron | | | |
| P(1)–B(3)–B(1) | 117.2(4) | [P(1)–B(3)–Rh(2) | 126.6(3)] |
| P(1)–B(3)–B(4) | 124.4(4) | | |
| P(1)–B(3)–B(6) | 120.7(3) | P(1)–B(3)–B(7) | 113.5(4) |
| P(2)–B(10)–B(6) | 129.0(4) | P(2)–B(10)–B(9) | 134.1(3) |
| P(2)–B(10)–B(7) | 121.9(4) | P(2)–B(10)–B(8) | 126.2(4) |

[2-($\eta^5$-$C_5Me_5$)-*closo*-2-$RhB_9H_7$-3,10-($PMe_2Ph$)$_2$]. Although the nickeladecaborane anions [2-($\eta^5$-$C_5H_5$)-*closo*-2-$NiB_9H_9$]$^-$ and [2-($\eta^5$-$C_5H_5$)-*closo*-2-$NiB_9Cl_9$]$^-$ have been known for several years,[27,28] compound (**3**) is the first *closo* metalladecaborane of conventional bicapped square antiprismatic 1:4:4:1 stack geometry to be structurally characterized that has the metal atom in the five-connected 2 position. Few *closo* metalladecaboranes of any kind have in fact been reported, the other previous examples being limited to the 1-metalla species [1,1-($PMe_2Ph$)$_2$-*closo*-1-$NiB_9H_7$-2,4-$Cl_2$],[29] [1-($\eta^5$-$C_5H_5$)-*closo*-1-$NiB_9H_9$],[27,28] and [1-($\eta^5$-$C_5H_5$)-*closo*-1-$NiB_9Cl_9$][27,28] (also of the 1:4:4:1 stack system), together with the '*isocloso*' 1-irida-,[13,30] 1-ferra-,[31] and 1-ruthenadecaboranes[32,33] of 1:3:3:3 stack geometry. The 2-metalla 1:4:4:1 stack configuration is however better recognized for metallamonocarbaborane and metalladicarbaborane clusters,[34–37] and in this context the electrolobal[10] equivalence of the B($PMe_2Ph$) and CH cluster fragments is in accord with this.

The rhodium–boron distances to B(3), B(5), B(6), and B(9) of 220.3(6)—226.1(6) pm are towards the centre of previously established ranges (refs. 1, 5—9, and Table 1), but that of 204.9(6) pm to the apical boron atom B(1) is at the extreme lower end. Although shorter distances to the apical atoms are a feature of $[B_{10}H_{10}]^{2-}$ and other *closo* ten-vertex $D_{4d}$-based structures,[9,38] the shrinkage of some 20 pm is somewhat greater than the mean shrinkage of *ca.* 10 pm in the B–B distances to the apical B(1) and B(10) atoms compared to the other interboron distances in the molecule, perhaps reflecting a greater bonding flexibility of rhodium *versus* boron. An interesting feature is the distance B(6)–B(9), which is long at *ca.* 200 pm, and therefore perhaps reminiscent of incipient *isonido*[4,9,13] character [which would require B(6)–B(9) of *ca.* 230—260 pm].

The B(3)–P(1) distance of 189.8(6) for the 'tropical' boron atom B(3) is towards the centre of previously observed ranges (*ca.* 186—198 pm)[9] for a pendant tertiary phosphine ligand on a metallaborane cluster, but the distance B(10)–P(2) involving the apical position is at the extreme low end of recorded ranges, probably reflecting high *s* character and a stronger bond to this phosphine as also manifested in the higher internuclear spin–spin coupling constant $^1J(^{31}P–^{11}B)$ of *ca.* 190 Hz for this position (Table 6 below). The equivalent correlation of $^1J(^{11}B–^1H)$ with boron *s* character, cage 'umbrella angle', *etc.*, is well recognized.[23,39–41]

As with compound (**2**) discussed above, the rhodium atom can be regarded as a six valence-orbital 18-electron $d^6$ octahedral rhodium(III) centre, and the molecule has sandwich character, with the dihedral angle between the mean cyclopentadienyl and B(1)B(3)B(5)B(6)B(9) planes being only 7°; the five methyl groups on the cyclopentadienyl ring are again bent *away* somewhat from the metal atom (range of angular deviation from the $C_5$ plane 2.5—5.1°).

The n.m.r. properties (Table 6 and Figure 4) are consistent with the molecular structure of Figure 3, thus confirming that the crystal was representative of the bulk sample. Likewise two-

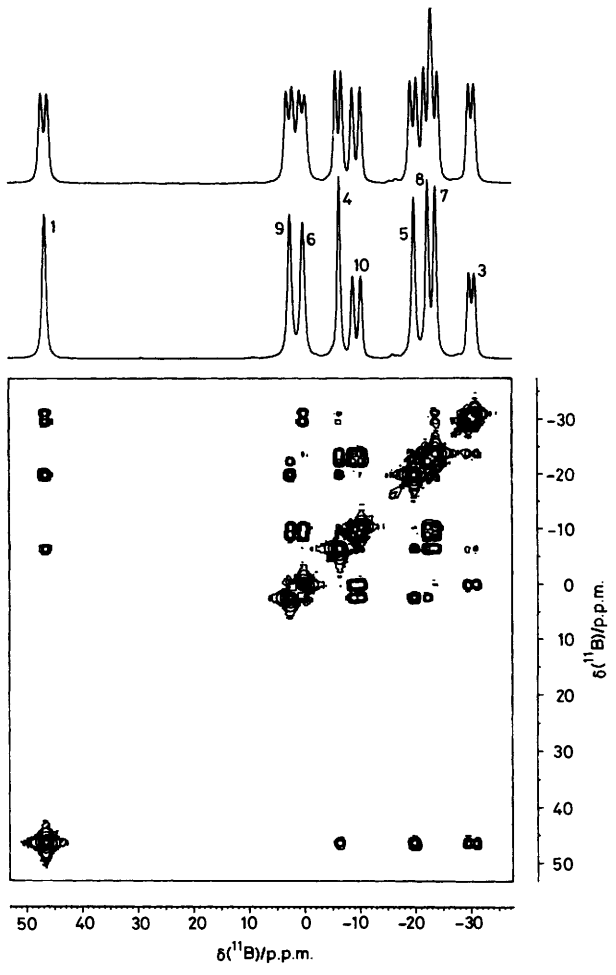


**Figure 4.** 128-MHz $^{11}B$ n.m.r. spectra of [2-($\eta^5$-$C_5Me_5$)-*closo*-2-$RhB_9H_7$-3,10-($PMe_2Ph)_2$] (**3**) in $C_6D_5CD_3$ solution at +90 °C. All except the uppermost trace were recorded under conditions of {$^1$H-(broad-band noise)} decoupling. The top two traces are straightforward $^{11}B$ spectra and the bottom diagram is an [$^{11}B$–$^{11}B$]-COSY 90 contour plot

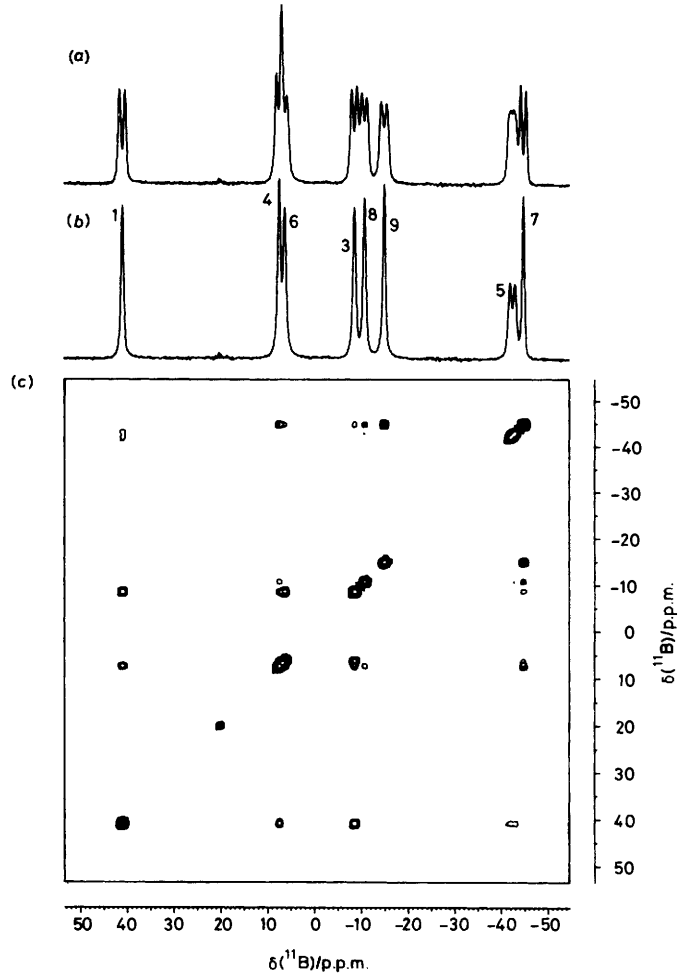


**Figure 5.** 128-MHz $^{11}B$ n.m.r. spectra of [2-($\eta^5$-$C_5Me_5$)-*nido*-2-$RhB_8H_{10}$-5-($PMe_2Ph$)] (**4**) in $C_6D_5CD_3$ solution at +90 °C. (*a*) Straightforward $^{11}B$ spectrum. (*b*) $^{11}B$ Spectrum recorded with {$^1$H(broad-band noise)} decoupling. (*c*) [$^{11}B$–$^{11}B$]-COSY 90 contour plot, for which data were collected under conditions of {$^1$H(broad-band noise)} decoupling

dimensional [$^{11}B$–$^{11}B$]-COSY[17–19] spectroscopy allied with $^1$H-{$^{11}$B(selective)}[20,21] experiments permitted the assignment of the $^{11}B$ and $^1$H resonances to their specific cluster positions. Interesting points again include the wide differential effect on the shielding of the boron nuclei α to the metal atom when compared to those[42] of the non-metalla borane analogue 1,6-($PMe_2Ph)_2$-*closo*-$B_{10}H_8$. Thus δ($^{11}$B) for B(3) and B(5) are almost unchanged, whereas for B(6) and B(9) there is a marked deshielding (Δσ *ca.* −25 p.p.m.) which is even greater for the apical B(1) atom [Δσ *ca.* −45 p.p.m.; *cf.* a similar shift for the B(1) position in compound (**4**), Table 7]. There are also substantial β effects at B(4) and B(10) (Δσ both *ca.* −15 p.p.m.), whereas the differential effect of the 3-($PMe_2Ph$) substituent only induces a 9 p.p.m. difference in δ($^{11}$B) between B(3) and B(5), the differential effect on the more distant B(6)B(9) and B(7)B(8) pairs being < *ca.* 1.5 p.p.m. in each case. A second interesting point is that in the two-dimensional [$^{11}B$–$^{11}B$]-COSY plot (Figure 4 and Table 6) couplings within a particular tropical belt are either weak or non-existent, whereas the interbelt correlations and the belt–axial correlations are strong, the exception to these latter being the somewhat weaker $^{11}B(5)$–$^{11}B(8)$ correlation. Some of the weaker correlations between closely spaced resonances [*e.g.* $^{11}B(7)$–$^{11}B(8)$] were only apparent on plots from COSY-45 experiments.

(d) *Characterization of* [2-($\eta^5$-$C_5Me_5$)-*nido*-2-$RhB_8H_{10}$-5-($PMe_2Ph$)] (**4**).—Compound (**4**) was more reluctant to crystallize than were (**2**) and (**3**) and, in addition, was less robust in solution, particularly in halogenated solvents. This has so far precluded our obtaining crystals suitable for a single-crystal *X*-ray diffraction analysis, but the identification of (**4**) readily follows from multielement, multiple resonance, and multi-dimensional n.m.r. spectroscopy (Table 7 and Figure 5). Thus $^{11}B$ n.m.r. indicates eight individual boron atoms. $^1$H-{$^{11}$B} experiments thence show that each, except one (which is bound to phosphorus), is bound to an *exo*-terminal hydrogen atom, and that there are in addition three bridging hydrogen atoms, of which one is at rather high field and associated with only one boron atom (and Rh). The extreme similarity of the overall $^{11}B$ and $^1$H cluster shielding pattern to those of the known nine-vertex *nido*-2-metallaboranes [2,2,2-(CO)($PMe_3)_2$-*nido*-2-$IrB_8H_{11}$][13,43] and [2,2,2,2,2-($PMe_2Ph)_3H_2$-*nido*-2-$ReB_8H_{11}$],[44] which are included in Table 7 for this comparison, reasonably identifies (**4**) also as a *nido*-2-metallanonaborane. A

**Table 6.** Measured n.m.r. parameters for [2-($\eta^5$-$C_5Me_5$)-*closo*-2-$RhB_9H_7$-3,10-($PMe_2Ph$)$_2$] (3)

| Assignment[a] | $\delta(^{11}B)$/p.p.m.[b] $CD_2Cl_2$ solution (294 K) | $\delta(^1H)$/p.p.m.[c] $CD_2Cl_2$ solution (294 K) | $^1J(^{11}B-^1H)$/Hz[d] $C_6D_5CD_3$ solution (383 K) | $\delta(^{11}B)$/p.p.m.[b] $C_6D_5CD_3$ solution (383 K) | Observed [$^{11}B-^{11}B$]-COSY correlations[e] $C_6D_5CD_3$ solution (383 K) |
|---|---|---|---|---|---|
| 1 | +44.6 | +6.27 | 150 | +46.5 | 3s 4s 5s |
| 2 | Rh position | $C_5Me_5$[f] | | | |
| 3 | −30.1[g] | $PMe_2Ph$[h] | | −30.3[g] | 1s 4vw? 6s 7w |
| 4 | −7.7 | +1.85 | 137 | −6.5 | 1s 3vw? 5w 7s 8s |
| 5 | −21.5 | −0.34 | 140 | −19.9 | 1s 4w 8w 9s |
| 6 | +0.1 | +2.36[i] | 132 | 0.0 | 3s 7vw? 10s |
| 7 | −24.3 | −0.16 | *ca.* 150[j] | −23.8 | 3w 4s 6vw? 8vw? 10s |
| 8 | −23.6 | −0.13 | *ca.* 150[j] | −22.4 | 4s 5w 7vw? 9w 10s |
| 9 | +1.5 | +2.22[k] | 146 | +2.4 | 5s 8w 10s |
| 10 | −8.7[l] | $PMe_2Ph$[h] | | −9.6[l] | 6s 7s 8s 9s |

[a] Assignment by P-substituted positions and two-dimensional [$^{11}B-^{11}B$]-COSY experiments. Numbering as in structure (II) and Figure 3. [b] ±0.5 p.p.m. to high frequency (low field) of $BF_3(OEt_2)$ in $CDCl_3$. [c] ±0.05 p.p.m. to high frequency (low field) of $SiMe_4$; $^1H$ resonances assigned to directly-bound B positions by selective $^1H-\{^{11}B\}$ experiments. [d] ±5 Hz; measured from $^{11}B$ spectra with resolution enhancement to achieve baseline separation of doublet components. [e] s = Strong, w = weak, vw = very weak; note that observed intensities will depend upon *both* $^1J(^{11}B-^{11}B)$ *and* $T_2^*$ ($^{11}B$) and therefore upon solution conditions. [f] $\delta(^1H)(C_5Me_5)$ +1.66 p.p.m. Fine structure apparent in 400-MHz $^1H-\{^{11}B$(broad-band noise)$\}$ spectrum under conditions of high resolution and with appropriate line-narrowing functions; doublet splittings 0.25 Hz [arising from $^5$ or $^6J(^{31}P-^1H)$ as confirmed by $^1H-\{^{31}P\}$ experiments] and 0.49 Hz [probably arising from $^3J(^{103}Rh-^1H)$, possibly $^5J(^1H-^1H)$]. [g] Doublet, splitting 128 ± 5 Hz due to $^1J(^{31}P-^{11}B)$(*exo*). [h] $^{31}P$ Spectrum shows two overlapping quartets centred at $\delta(^{31}P)$ *ca.* 0.15 (splitting *ca.* 130 Hz) and −1.75 p.p.m. (splitting *ca.* 180 Hz) in $CD_2Cl_2$ solution at 294 K (δ w.r.t. 85% $H_3PO_4$); $^1H$ spectrum shows four independent P-methyl resonances [B(3) and B(10) are chiral centres] at $\delta(^1H)$ +2.07, +2.05 [each with $^2J(^{31}P-^1H)$ *ca.* 11.9 Hz to $\delta(^{31}P)$ −1.75 p.p.m.], +1.60, +1.50 [each with $^2J(^{31}P-C-^1H)$ *ca.* 11.5 Hz to $\delta(^{31}P)$ −0.15 p.p.m.], plus aromatic $^1H$ resonances at $\delta(^1H)$ 7.4—7.6 and 8.1—8.2 p.p.m. [i] Doublet in $^1H-\{^{11}B$(broad-band noise)$\}$ spectrum, splitting 19 Hz probably due to $^3J(^{31}P-B-B-^1H)$ rather than $^2J(^{103}Rh-^1H)$. [j] Overlapping $^{11}B(7)$ and $^{11}B(8)$ resonances preclude more accurate estimation. [k] Possible doublet in $^1H-\{^{11}B$(broad-band noise)$\}$ spectrum, probably due to $^3J(^{31}P-B-B-^1H)$. [l] Doublet, splitting 188 ± 5 Hz due to $^1J(^{31}P-^{11}B)$.

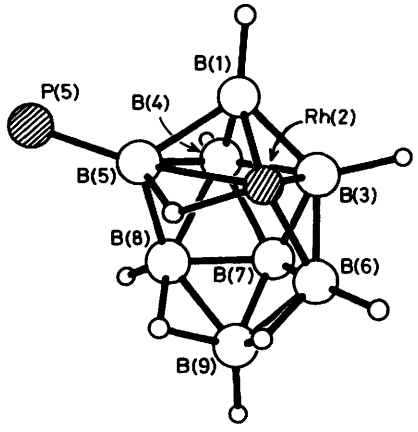


**Figure 6.** Representation of the proposed structure of compound (4), *viz.* [2-($\eta^5$-$C_5Me_5$)-*nido*-$RhB_8H_{10}$-5-($PMe_2Ph$)], with organyl carbon and hydrogen atoms omitted. In this projection the *exo*-terminal hydrogen atom on B(7) is obscured

more detailed consideration of the n.m.r. parameters summarized in Table 7 readily established the structural formulation as [2-($\eta^5$-$C_5Me_5$)-*nido*-2-$RhB_8H_{10}$-5-($PMe_2Ph$)], the assignments and connectivities among the boron atoms in the cluster being established by two-dimensional [$^{11}B-^{11}B$]-COSY[17-19] spectroscopy (Figure 5), which also thereby confirmed the skeletal type. A representation of the cluster structure is drawn in Figure 6.

The compound can be regarded as a direct structural analogue of the *nido*-$[B_9H_{12}]^-$ anion (itself only recently characterized structurally)[45] in which, formally, (*a*) a neutral BH unit at the 2 position has been notionally replaced by the isoelectronic and isolobal neutral $Rh(C_5Me_5)$ moiety, and (*b*) an anionic $BH^-$ unit at the adjacent 5 position has been replaced by the isoelectronic and isolobal neutral $B(PMe_2Ph)$ moiety. As with compounds (1)—(3) the metal centre can be regarded as 18-electron, six valence-orbital, octahedral $d^6$ rhodium(III), and there is sandwich character between the $\eta^5$-$C_5$ and B(1)B(3)B(5)B(6) faces.

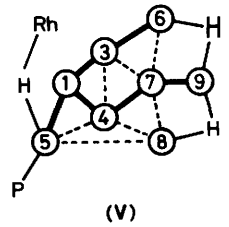


(V)

Detailed n.m.r. shielding considerations in (4) and the other known *nido*-2-metallanonaboranes are to be presented elsewhere,[44] although, as with compounds (1)—(3), the wide variation in cluster shielding induced by the subrogation of the $Rh(C_5Me_5)$ centre into the basic $[B_9H_{12}]^-$ skeleton is again noteworthy, with the $\Delta\sigma(\alpha)$ effects at B(1), B(3), B(5), and B(6) being *ca.* −49, +1, +9, and −17 p.p.m. respectively, and the transannular[46] $\Delta\sigma(\beta)$ effect at B(4) being marked at −16 p.p.m. A second interesting shielding phenomenon is the high shielding for the Rh(2)–H–B(5) bridging proton, as also observed for the iridium[43] and rhenium[44] congeners. High shielding in this position is also observed for the corresponding B(2)–H–B(5) link in $[B_9H_{12}]^-$, however,[43-45] and so there is now no need to invoke terminal M–H bond character to account for this as we tentatively entertained for the iridium analogue.[43] Aspects of the two-dimensional [$^{11}B-^{11}B$]-COSY results are also noteworthy.[44] Correlations [represented in structure (V)] were observed for all pairs of adjacent boron atoms except for the hydrogen-bridged B(6)B(9) and B(8)B(9) linkages.

**Table 7.** Measured n.m.r. data for [2-($\eta^5$-$C_5Me_5$)-*nido*-2-$RhB_8H_{10}$-5-($PMe_2Ph$)] (**4**)[a] together with data for [2,2,2-(CO)($PMe_3$)$_2$-*nido*-2-$IrB_8H_{11}$][b] and [2,2,2,2,2-($PMe_2Ph$)$_3H_2$-*nido*-2-$ReB_8H_{11}$][c] for comparison

| | [2-($\eta^5$-$C_5Me_5$)-*nido*-2-$RhB_8H_{10}$-5-($PMe_2Ph$)] (**4**)[a] | | | | | [(CO)($PMe_3$)$_2$$IrB_8H_{11}$][b] $CDCl_3$ solution (294 K) | | [($PMe_2Ph$)$_3H_2$$ReB_8H_{11}$][c] $CD_2Cl_2$ solution (294 K) | |
|---|---|---|---|---|---|---|---|---|---|
| Assignment[d] | $\delta(^{11}B)$/p.p.m.[e] $CDCl_3$ solution (294 K) | $\delta(^1H)$/p.p.m.[f] $CDCl_3$ solution (294 K) | $^1J(^{11}B-^1H)$/Hz[g] $C_6D_5CD_3$ solution (383 K) | $\delta(^{11}B)$/p.p.m. $C_6D_5CD_3$ solution (383 K) | Observed [$^{11}B$–$^{11}B$]-COSY correlations[h] $C_6D_5CD_3$ solution (383 K) | $\delta(^{11}B)$/p.p.m.[e] | $\delta(^1H)$/p.p.m.[f] | $\delta(^{11}B)$/p.p.m.[e] | $\delta(^1H)$/p.p.m.[f] |
| 1 | +39.4 | +5.82 | 154 | +40.8 | 3s 4s 5s | +23.1 | +5.04 | +28.9 | +5.26 |
| 2 | Rh position | $C_5Me_5$[i] | | Rh position | | Ir position | | Re position | |
| 3 | −10.7 | +0.95 | 142 | −8.8 | 1s 4w 6s 7w | −15.3 | +0.83 | −18.3 | +0.17 |
| 4 | +5.3 | +3.26[j] | *ca.* 150[k] | +7.3 | 1s 3w 5vw? 7s 8w | +8.8 | +4.90 | +7.9 | +4.14 |
| 5 | −42.8[l] | $PMe_2Ph$[l] | | −42.5[l] | 1s 4vw? 8vw | −39.9 | −0.51 | −46.3 | −0.30 |
| 6 | +3.9 | +2.55[j] | *ca.* 155[k] | +6.1 | 3s 7w | −5.3 | +2.94 | −5.0 | +2.73 |
| 7 | −46.2 | −0.95 | 144 | −44.9 | 3w 4s 6w 8w 9s | −52.5 | −1.48 | −53.2 | −1.39 |
| 8 | −12.3 | +1.50 | 141 | −10.9 | 4s 5vw 7w | −13.6 | +1.02 | −16.5 | +0.83 |
| 9 | −16.6 | +2.78 | 157 | −15.1 | 7s | −14.5 | +2.99 | −16.0 | +2.42 |
| 2,5 (bridge) | | −13.60[m,n] | 58 | | | | −14.50 | | −14.09 |
| 6,9 (bridge) | | −0.37[o] | *p* | | | | −2.10 | | −3.81 |
| 8.9 (bridge) | | −2.63[q] | *p* | | | | −2.96 | | −3.89 |

[a] This work. [b] Data from ref. 43. [c] Data from ref. 44. [d] Assignment by $^1H$-{$^{11}B$} and two-dimensional [$^{11}B$–$^{11}B$]-COSY spectroscopy (see also ref. 44). Numbering as in structure (**III**) and Figure 6. [e] ±0.5 p.p.m. to high frequency (low field) of $BF_3(OEt_2)$ in $CDCl_3$. [f] ±0.05 p.p.m. to high frequency (low field) of $SiMe_4$; $^1H$ resonances related to directly-bound B positions by selective $^1H$-{$^{11}B$} experiments, $^1H$ at 100 and $^{11}B$ at 32 MHz. [g] ±5 Hz; measured from $^{11}B$ spectra with resolution enhancement to achieve baseline separation of doublet components. [h] s = Strong, w = weak, vw = very weak; note that observed intensities will depend on *both* $^1J(^{11}B-^{11}B)$ and $T_2^*(^{11}B)$ and therefore upon solution conditions. [i] $\delta(^1H)(C_5Me_5)$ *ca.* +1.78 p.p.m. [j] Some uncertainty as to the assignment of these between $^1H(4)$ and $^1H(6)$ since partial overlap of $^{11}B(4)$ and $^{11}B(6)$ precluded good selectivity in $^1H$-{$^{11}B$} experiments. [k] More accurate assessment prevented by partially overlapping $^{11}B(4)$ and $^{11}B(6)$ resonances. [l] $^1J(^{31}P-^{11}B)(exo)$ 143 Hz. [m] Selectively sharpened by $\nu[^{11}B(5)]$ in $^1H$-{$^{11}B$} experiments. [n] Splitting of 25 Hz apparent in $^1H$-{$^{11}B$(broad-band noise)} spectrum, arising from either $^1J(^{103}Rh-^1H)$ or $^2J(^{31}P-B-^1H)$. [o] Selectively sharpened by $\nu[^{11}B(9)]$ strongly and $\nu[^{11}B(6)]$ weakly in $^1H$-{$^{11}B$(selective)} experiments. [p] Not resolved. [q] Selectively sharpened by $\nu[^{11}B(9)]$ strongly and $\nu[^{11}B(8)]$ weakly in $^1H$-{$^{11}B$(selective)} experiments.

**Table 8.** Atom co-ordinates ( $\times 10^4$) for compound (2)

| Atom | *x* | *y* | *z* | Atom | *x* | *y* | *z* |
|---|---|---|---|---|---|---|---|
| Rh(5) | 3 484.3(2) | 4 224.5(3) | 1 612.9(1) | H(12B) | 6 903(5) | 5 800(5) | 5 526(2) |
| P(1) | 7 224(1) | 6 854(1) | 4 246(1) | H(12C) | 8 500(5) | 7 137(5) | 5 782(2) |
| C(11) | 5 972(4) | 8 312(4) | 4 465(3) | H(132) | 7 435(2) | 8 853(3) | 2 969(1) |
| C(12) | 7 888(5) | 6 188(5) | 5 298(2) | H(133) | 9 540(2) | 10 165(3) | 2 616(1) |
| C(131) | 8 772(2) | 7 841(3) | 4 020(1) | H(134) | 12 063(2) | 9 893(3) | 3 468(1) |
| C(132) | 8 536(2) | 8 734(3) | 3 340(1) | H(135) | 12 482(2) | 8 308(3) | 4 673(1) |
| C(133) | 9 722(2) | 9 474(3) | 3 142(1) | H(136) | 10 377(2) | 6 996(3) | 5 026(1) |
| C(134) | 11 145(2) | 9 320(3) | 3 622(1) | H(6A) | 2 764(5) | 8 170(5) | 1 286(3) |
| C(135) | 11 381(2) | 8 427(3) | 4 301(1) | H(6B) | 1 939(5) | 7 774(5) | 2 140(3) |
| C(136) | 10 195(2) | 7 687(3) | 4 500(1) | H(6C) | 842(5) | 7 884(5) | 1 073(3) |
| C(1) | 1 810(3) | 5 810(4) | 1 115(2) | H(7A) | 3 485(5) | 4 993(7) | −577(3) |
| C(2) | 2 326(4) | 5 074(5) | 386(2) | H(7B) | 3 929(5) | 6 729(7) | 203(3) |
| C(3) | 1 991(4) | 3 462(5) | 263(2) | H(7C) | 2 280(5) | 6 503(7) | −634(3) |
| C(4) | 1 267(4) | 3 188(4) | 939(2) | H(8A) | 2 500(6) | 1 236(7) | −161(3) |
| C(5) | 1 160(3) | 4 651(4) | 1 465(2) | H(8B) | 3 244(6) | 2 604(7) | −682(3) |
| C(6) | 1 873(5) | 7 534(5) | 1 431(3) | H(8C) | 1 367(6) | 1 993(7) | −1 042(3) |
| C(7) | 3 046(5) | 5 914(7) | −190(3) | H(9A) | 1 200(5) | 736(5) | 783(4) |
| C(8) | 2 288(6) | 2 254(7) | −470(3) | H(9B) | −517(5) | 1 538(5) | 694(4) |
| C(9) | 619(5) | 1 665(5) | 1 056(4) | H(9C) | 691(5) | 1 622(5) | 1 752(4) |
| C(10) | 407(4) | 4 927(5) | 2 217(3) | H(10A) | 414(4) | 3 817(5) | 2 437(3) |
| B(1) | 3 949(4) | 2 903(5) | 2 727(3) | H(10B) | −711(4) | 5 224(5) | 1 995(3) |
| B(2) | 4 317(4) | 4 941(4) | 3 067(2) | H(10C) | 983(4) | 5 803(5) | 2 764(3) |
| B(3) | 5 492(4) | 3 677(5) | 3 594(3) | H(1) | 3 025(34) | 2 376(35) | 2 867(20) |
| B(4) | 5 615(5) | 1 915(5) | 2 886(3) | H(2) | 3 606(33) | 5 583(35) | 3 442(20) |
| B(6) | 5 298(4) | 5 831(5) | 2 376(3) | H(3) | 5 811(42) | 3 604(45) | 4 393(26) |
| B(7) | 6 252(4) | 5 265(4) | 3 291(2) | H(4) | 5 780(48) | 746(47) | 3 199(27) |
| B(8) | 7 071(5) | 3 456(5) | 3 109(3) | H(6) | 5 361(37) | 6 949(44) | 2 286(23) |
| B(9) | 6 529(5) | 2 052(5) | 2 070(3) | H(8) | 8 263(36) | 3 297(37) | 3 519(21) |
| B(10) | 4 567(5) | 1 983(5) | 1 797(3) | H(9) | 7 299(43) | 1 176(45) | 1 864(25) |
| H(11A) | 5 666(4) | 8 845(4) | 3 875(3) | H(10) | 4 001(49) | 1 014(54) | 1 364(30) |
| H(11B) | 8 515(4) | 9 178(4) | 5 027(3) | H(5,6) | 5 108(60) | 5 058(65) | 1 689(37) |
| H(11C) | 5 002(4) | 7 813(4) | 4 601(3) | H(8,9) | 7 160(45) | 3 284(49) | 2 227(27) |
| H(12A) | 8 586(5) | 5 243(5) | 5 218(2) | H(9,10) | 5 632(40) | 2 414(42) | 1 437(24) |

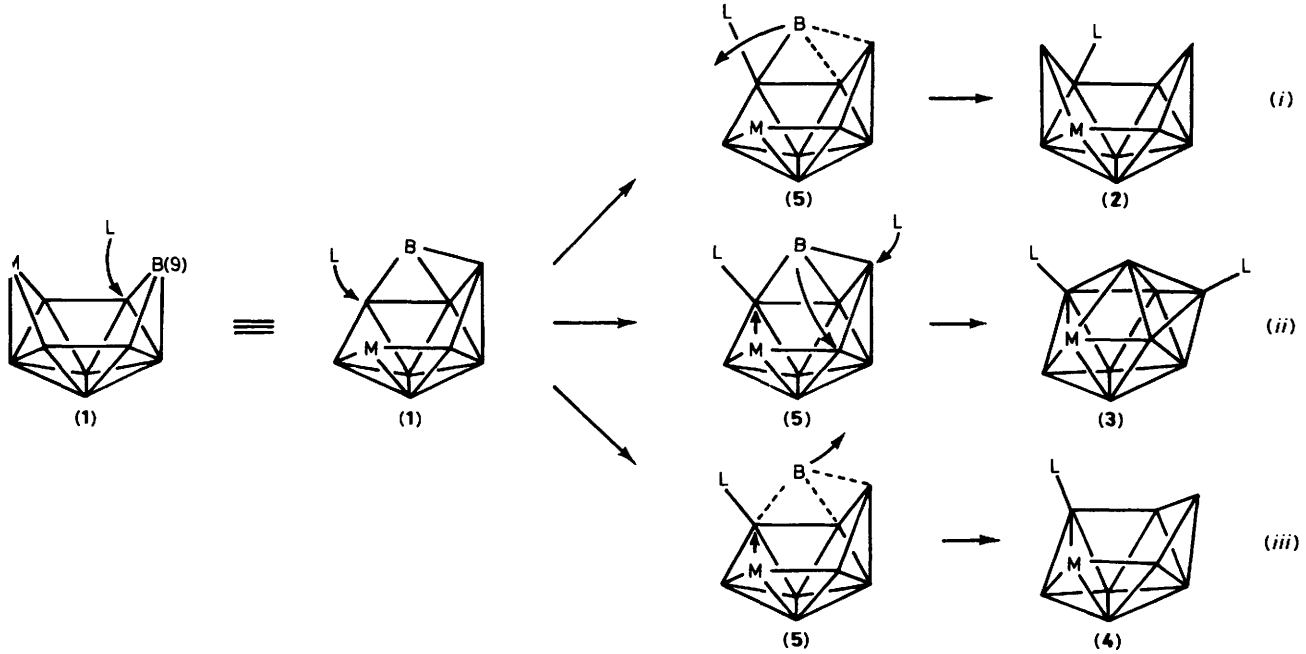


**Scheme 2.**

(e) *Mechanism of Formation of Compounds* (2)—(4).—The aggregated yield of the three products of the reaction is high (60—70%), and the fact that all are still formed (though more slowly) in similar proportions when a deficiency of phosphine is used suggests that their formations are competitive rather than sequential. The three idealized reaction stoicheiometries are given in equations (1)—(3). The '$BH_3$' eliminated in equation (3) may well be sequestered as $BH_3(PMe_2Ph)$ since n.m.r.

**Table 9.** Atom co-ordinates ( $\times 10^4$) for compound (3)

| Atom | *x* | *y* | *z* | Atom | *x* | *y* | *z* |
|---|---|---|---|---|---|---|---|
| Rh(2) | 1 735.0(2) | 324.4(2) | 3 310.7(1) | H(12A) | 1 394(4) | −2 400(4) | 4 513(2) |
| P(1) | 1 967(1) | −2 665(1) | 3 281(1) | H(12B) | 1 546(4) | −3 782(4) | 4 296(2) |
| P(2) | 2 465(1) | −24(1) | 637(1) | H(12C) | 581(4) | −3 047(4) | 3 870(2) |
| C(11) | 3 205(3) | −2 643(4) | 3 603(3) | H(132) | 3 299(2) | −4 199(2) | 2 653(2) |
| C(12) | 1 318(4) | −3 000(4) | 4 078(2) | H(133) | 3 021(2) | −5 787(2) | 1 829(2) |
| C(131) | 1 811(2) | −3 823(2) | 2 685(2) | H(134) | 1 376(2) | −6 305(2) | 1 396(2) |
| C(132) | 2 581(2) | −4 425(2) | 2 464(2) | H(135) | 8(2) | −5 236(2) | 1 787(2) |
| C(133) | 2 425(2) | −5 320(2) | 2 000(2) | H(136) | 287(2) | −3 648(2) | 2 611(2) |
| C(134) | 1 497(2) | −5 613(2) | 1 756(2) | H(21A) | 3 507(4) | −1 431(4) | 911(3) |
| C(135) | 726(2) | −5 010(2) | 1 976(2) | H(21B) | 3 477(4) | −1 119(3) | −50(3) |
| C(136) | 883(2) | −4 115(2) | 2 440(2) | H(21C) | 2 541(4) | −1 915(4) | 330(3) |
| C(21) | 3 050(4) | −1 263(4) | 421(3) | H(22A) | 1 077(3) | −356(4) | −133(2) |
| C(22) | 1 627(3) | 255(4) | −143(2) | H(22B) | 1 919(3) | 255(4) | −678(2) |
| C(231) | 3 348(2) | 1 025(2) | 614(1) | H(22C) | 1 325(3) | 1 043(4) | −41(2) |
| C(232) | 3 775(2) | 1 268(2) | −38(1) | H(232) | 3 567(2) | 832(2) | −540(1) |
| C(233) | 4 471(2) | 2 075(2) | −41(1) | H(233) | 4 801(2) | 2 264(2) | −546(1) |
| C(234) | 4 740(2) | 2 639(2) | 608(1) | H(234) | 5 278(2) | 3 264(2) | 605(1) |
| C(235) | 4 313(2) | 2 396(2) | 1 260(1) | H(235) | 4 521(2) | 2 833(2) | 1 762(1) |
| C(236) | 3 617(2) | 1 589(2) | 1 263(1) | H(236) | 3 287(2) | 1 401(2) | 1 768(1) |
| C(1) | 2 174(3) | 471(3) | 4 522(2) | H(6A) | 2 586(3) | −1 046(4) | 4 940(2) |
| C(2) | 1 459(2) | 1 248(3) | 4 334(2) | H(6B) | 1 414(3) | −700(4) | 5 138(2) |
| C(3) | 1 811(2) | 1 968(3) | 3 802(2) | H(6C) | 2 393(3) | −82(4) | 5 634(2) |
| C(4) | 2 760(2) | 1 663(3) | 3 674(2) | H(7A) | 448(3) | 730(4) | 5 062(2) |
| C(5) | 2 983(3) | 731(3) | 4 107(2) | H(7B) | −93(3) | 1 275(4) | 4 236(2) |
| C(6) | 2 129(3) | −396(4) | 5 102(2) | H(7C) | 475(3) | 2 142(4) | 4 905(2) |
| C(7) | 498(3) | 1 353(4) | 4 647(2) | H(8A) | 1 818(3) | 3 396(3) | 3 202(2) |
| C(8) | 1 290(3) | 2 948(3) | 3 482(2) | H(8B) | 996(3) | 3 461(3) | 3 892(2) |
| C(9) | 3 423(3) | 2 269(4) | 3 212(2) | H(8C) | 727(3) | 2 691(3) | 3 085(2) |
| C(10) | 3 951(3) | 197(4) | 4 186(3) | H(9A) | 3 000(3) | 2 643(4) | 2 762(2) |
| B(1) | 591(3) | −706(4) | 3 196(2) | H(9B) | 3 954(3) | 1 749(4) | 2 993(2) |
| B(3) | 1 543(3) | −1 342(4) | 2 833(2) | H(9C) | 3 772(3) | 2 891(4) | 3 552(2) |
| B(4) | 405(3) | −1 165(4) | 2 311(2) | H(10A) | 3 905(3) | −516(4) | 4 528(3) |
| B(5) | 412(3) | 289(4) | 2 527(2) | H(10B) | 4 462(3) | 756(4) | 4 446(3) |
| B(6) | 2 362(3) | −477(3) | 2 372(2) | H(10C) | 4 176(3) | −36(4) | 3 650(3) |
| B(7) | 1 486(3) | −1 336(4) | 1 839(2) | H(1) | 146(22) | −947(27) | 3 624(18) |
| B(8) | 688(3) | −185(4) | 1 625(2) | H(4) | −207(22) | −1 787(28) | 2 175(17) |
| B(9) | 1 485(3) | 770(4) | 2 133(2) | H(5) | −241(21) | 872(27) | 2 582(17) |
| B(10) | 1 878(3) | −138(4) | 1 528(2) | H(6) | 3 159(27) | −592(32) | 2 442(21) |
| H(11A) | 3 307(3) | −2 011(4) | 4 014(3) | H(7) | 1 594(20) | −2 087(28) | 1 564(16) |
| H(11B) | 3 593(3) | −2 441(4) | 3 128(3) | H(8) | 97(25) | −53(29) | 1 130(20) |
| H(11C) | 3 463(3) | −3 405(4) | 3 834(3) | H(9) | 1 579(23) | 1 600(31) | 2 030(19) |

spectroscopy shows that the latter is present in the product mixture.

$$[(C_5Me_5)RhB_9H_{13}]\ (1) + PMe_2Ph \longrightarrow [(C_5Me_5)RhB_9H_{11}(PMe_2Ph)]\ (2) + H_2 \quad (1)$$

$$[(C_5Me_5)RhB_9H_{13}]\ (1) + 2PMe_2Ph \longrightarrow [(C_5Me_5)RhB_9H_7(PMe_2Ph)_2]\ (3) + 3H_2 \quad (2)$$

$$[(C_5Me_5)RhB_9H_{13}]\ (1) + PMe_2Ph \longrightarrow [(C_5Me_5)RhB_8H_{10}(PMe_2Ph)]\ (4) + \text{'}BH_3\text{'} \quad (3)$$

The geometrical disposition of the phosphine ligands in the products makes it tempting to entertain a possible mechanism of formation that involves a common intermediate (**5**) as shown schematically in Scheme 2 [equations (*i*)—(*iii*)].[3] In this scheme a phosphine ligand attacks at the B(10) position on the *nido*-6-metalladecaborane (**1**) and the adjacent B(9) vertex is labilized. This is then followed by: (*a*) a vertex swing[8,9,47] of B(9) towards B(5) to give the ten-vertex *nido*-5-metalladecaborane product (**2**) [equation (*i*)], (*b*) a swing of B(9) towards B(7) accompanied by M(6)–B(10) closure to give the ten-vertex *closo* compound (**3**) [equation (*ii*)], or (*c*) a loss of B(9) accompanied by M(6)–B(10) closure to give the nine-vertex *nido* species (**4**) [equation (*iii*)]. The proposed vertex-swing reaction of (*i*) and (*ii*) also occurs for [6-($\eta^6$-$C_6Me_6$)-*nido*-6-$RuB_9H_{13}$] though here the formation of [5-($\eta^6$-$C_6Me_6$)-*nido*-5-$RuB_9H_{11}$-7-($PMe_2Ph$)] is essentially quantitative with only trace amounts if any of any other metallaborane products.[33] By contrast, those Lewis-base adducts in the *nido*-6-mangana- and *nido*-6-rhenadecaborane systems that have so far been reported have retained their *nido*-6-metalladecaborane configurations,[48–51] even though they are believed also to undergo vertex-swing rearrangements.[48–50]

(f) *Additional N.M.R. Considerations.*—For the three compounds (**2**)—(**4**), a plot of $\delta(^1H)$ *versus* $\delta(^{11}B)$ for directly bound atoms is given in Figure 7, which also includes data [1] for the *nido*-6-rhodadecaborane (**1**) for completeness. It is apparent that there is an overall correlation with a slope $\delta(^1H):\delta(^{11}B)$ of 1: *ca.* 16 (solid line) for the *exo*-terminal protons, the maximum deviation from the line being *ca.* 1.5 p.p.m. in $\delta(^1H)$. Although this magnitude of deviation is of the order expected from local anisotropy variations, *etc.*, it is nevertheless now becoming evident[44,52] that a detailed consideration of these deviations in closely related series of compounds can constitute a structural diagnostic that is finding increasing use.[44,52]

The *exo*-proton data for the three different structure types, *viz. nido* ten-vertex (**1**) and (**2**), *closo* ten-vertex (**3**), and *nido* nine-

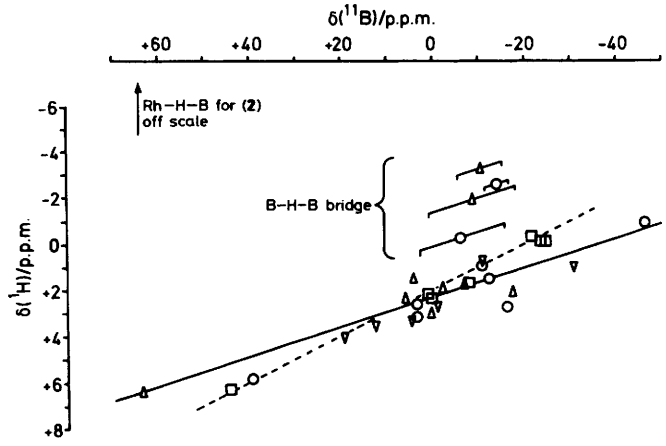


**Figure 7.** Proton–boron-11 shielding correlation plot for hydrogen atoms and their directly-bound boron atoms in compounds (**1**) (▽), (**2**) (△), (**3**) (□), and (**4**) (○). The solid line drawn has slope $\delta(^1H):\delta(^{11}B)$ *ca.* 1:16, and the dashed line slope *ca.* 1:12

vertex (**4**), all conform reasonably closely to the slope of 1:16 (solid line in Figure 7), although the data for the *closo* compound (**3**) correlate better with a somewhat steeper slope [dashed line in Figure 7; slope $\delta(^1H):\delta(^{11}B)$, 1:12, maximum deviation 0.4 p.p.m. in $\delta(^1H)$]. Insufficient comparison data are available to say whether this constitutes a general diagnostic for *closo* ten-vertex compounds; we note, moreover, that smaller five- and six-vertex ruthena- and osma-borane clusters also exhibit $\delta(^1H)(exo):\delta(^{11}B)$ gradients of *ca.* 1:12 whereas larger *nido*-type species conform more closely to the 1:16 relationship.[11,53,54]

## Experimental

*Reaction of* $[6\text{-}(\eta^5\text{-}C_5Me_5)\text{-}6\text{-}RhB_9H_{13}]$ (**1**) *with* $PMe_2Ph$ *and the Isolation of Compounds* (**2**)—(**4**).—$[6\text{-}(\eta^5\text{-}C_5Me_5)\text{-}6\text{-}RhB_9H_{13}]$ (**1**), prepared as in ref. 1 (0.30 g, 0.87 mmol), was dissolved in dry $CH_2Cl_2$ (30 $cm^3$) under dry $N_2$; $PMe_2Ph$ (*ca.* 0.3 g, 2.2 mmol) was then added and the solution stirred for 30 min at room temperature. During this time all the starting metallaborane (**1**) was consumed (analytical t.l.c.). The reaction mixture was then evaporated to dryness (rotary evaporator, $T \leqslant$ *ca.* 50 °C) and the residue redissolved in dry $CH_2Cl_2$ (5 $cm^3$). The resulting solution was then applied to a series of preparative t.l.c. plates [1-mm layer of silica (Kieselgel type GF54; Fluka) deposited on 200 × 200 mm glass formers from an acetone slurry followed by drying in air at 100 °C], and developed with $CH_2Cl_2$–hexane (3:1). Three main coloured bands were observed, with $R_f$ values of 0.54 (red-orange), 0.36 (orange), and $\leqslant$*ca.* 0.1 (yellow). These were removed from the plates, and separated from the silica by washing with dry $CH_2Cl_2$ (*ca.* 20 $cm^3$ per component). Repeated chromatography of each component using the same solvent system then yielded each in a pure state as a microcrystalline air-stable solid. The first compound ($R_f$ 0.54) was identified by *X*-ray crystallography as $[5\text{-}(\eta^5\text{-}C_5Me_5)\text{-}nido\text{-}5\text{-}RhB_9H_{11}\text{-}7\text{-}(PMe_2Ph)]$ (**2**) (0.15 g, 0.31 mmol, 35%). The second ($R_f$ 0.36) was identified by n.m.r. spectroscopy as $[2\text{-}(\eta^5\text{-}C_5Me_5)\text{-}nido\text{-}2\text{-}RhB_8H_{10}\text{-}5\text{-}(PMe_2Ph)]$ (**4**) (0.03 g, 0.063 mmol, 7.3%). The third compound, of low chromatographic mobility ($R_f \leqslant$ *ca.* 0.1), was identified by *X*-ray crystallography as $[2\text{-}(\eta^5\text{-}C_5Me_5)\text{-}closo\text{-}2\text{-}RhB_9H_7\text{-}3,10\text{-}(PMe_2Ph)_2]$ (**3**) (0.135 g, 0.22 mmol, 25%). Crystals of (**2**) and (**3**) suitable for the *X*-ray diffraction experiments (see later) were grown by slow evaporation of solutions in dry diethyl ether.

A similar reaction mixture was prepared from equimolar quantities of compound (**1**) (0.055 g, 0.16 mmol) and $PMe_2Ph$ (0.0218 g, 0.16 mmol) in $CD_2Cl_2$ solution (3.5 $cm^3$). An aliquot of this was transferred to a 10-mm outside-diameter n.m.r. tube and the reaction monitored by $^{11}B$ n.m.r. spectroscopy. After 3 h the n.m.r. spectrum showed the presence of compounds (**2**), (**3**), and (**4**) as well as the starting compound (**1**). Much overlap occurred in the centre of the spectrum [$\delta(^{11}B)$ +25 to −30 p.p.m.], but peaks due to compounds (**1**)—(**4**) and to $BH_3(PMe_2Ph)$ that were free from overlap at 128 MHz were at $\delta(^{11}B)$ +19.4, +64.0, +44.6, +39.4, and −37.7 p.p.m. respectively, integrating in the respective proportions 59.4 [2 B, compound (**1**)]:6.6 (**2**):16.0 (**3**):2.3 (**4**):3.0 [$BH_3(PMe_2Ph)$]. Many other resonance peaks of low intensity were also present: those in the central crowded region of the spectrum could not be distinguished, but separated isolated peaks towards the low-field end of the spectrum had the following $\delta(^{11}B)$ values [approx. intensities in parentheses, relative to compound (**3**) at 16.0]: +35.5 (2.6), +48.8 (1.2), +52.7 (1.8), +55.4 (2.8), and +66.9 (1.3). After 24 h the solution did not have a significantly different 128 MHz $^{11}B$ spectrum.

*Single-crystal X-Ray Diffraction Analyses.*—Intensity data for both (**1**) and (**2**) were collected on a Syntex $P2_1$ diffractometer operating in the ω–2θ scan mode using graphite-monochromated Mo-$K_\alpha$ radiation (λ = 71.069 pm) following a standard procedure.[55] The data sets for both compounds were corrected for absorption empirically once the structures had been determined.[56] Both compounds were solved *via* standard heavy-atom techniques and refined by full-matrix least squares using the SHELX program system.[57] Refinement for both compounds was essentially the same with all non-hydrogen atoms assigned anisotropic thermal parameters and phenyl groups included in the refinement as rigid groups with regular hexagonal geometry (C–C = 139.5 pm). All phenyl and methyl hydrogen atoms were included in calculated positions (C–H = 108 pm) and were assigned to an overall isotropic thermal parameter for each ligand. All the remaining hydrogen atoms were located in Fourier difference maps and were freely refined with individual isotropic thermal parameters. The weighting scheme $w = [\sigma^2(F_o) + g(F_o)^2]^{-1}$ was used for both compounds with the parameter *g* included in refinement to give a flat analysis of variance with increasing sinθ and $(F/F_{max})^{\frac{1}{2}}$. Atomic co-ordinates for (**2**) and (**3**) are given in Tables 8 and 9 respectively.

*Crystal data for compound* (**2**). $C_{18}H_{37}B_9PRh$, $M$ = 484.67, triclinic, $a$ = 940.9(2), $b$ = 875.2(2), $c$ = 1 561.4(2) pm, α = 99.06(2), β = 103.45(1), γ = 91.57(2)°, $U$ = 1.232 $nm^3$, $Z$ = 2, space group $P\bar{1}$, $D_c$ = 1.31 g $cm^{-3}$, μ(Mo-$K_\alpha$) = 6.80 $cm^{-1}$, $F(000)$ = 476.

*Data collection.* Scans running from 1° below $K_{\alpha1}$ to 1° above $K_{\alpha2}$, scan speeds 2.0—29.3° $min^{-1}$, $4.0 \leqslant 2\theta \leqslant 45.0°$. 3 186 Unique data, 3 080 [$I > 2.0\sigma(I)$] observed, $T$ = 290 K.

*Structure refinement.* Number of parameters = 317, weighting factor $g$ = 0.0002, $R$ = 0.0297, $R'$ = 0.0317.

*Crystal data for compound* (**3**). $C_{26}H_{48}B_9P_2Rh$, $M$ = 618.79, monoclinic, $a$ = 1 406.4(3), $b$ = 1 231.7(3), $c$ = 1 812.3(3) pm, β = 94.01(1)°, $U$ = 3.131 $nm^3$, $Z$ = 4, space group $P2_1/a$ (= $P2_1/c$, no. 14), $D_c$ = 1.31 g $cm^{-3}$, μ(Mo-$K_\alpha$) = 5.89 $cm^{-1}$, $F(000)$ = 1 260.

*Data collection.* Parameters as above. 3 893 Unique data, 3 530 observed [$I > 2.0\sigma(I)$].

*Structure refinement.* Number of parameters = 377, weighting factor $g$ = 0.000 35, $R$ = 0.0303, $R'$ = 0.0322.

*Nuclear Magnetic Resonance Spectroscopy.*—100-MHz $^1H$ and 32-MHz $^{11}B$ single and multiple resonance experiments were performed on a JEOL FX-100 spectrometer using general

techniques described elsewhere.[20,21,58–60] Some $^{1}H$-$\{^{11}B\}$ experiments were carried out at 360 MHz on a Bruker WH-360 instrument (S.E.R.C. service, University of Edinburgh), use being made of the technique[21,61] in which a $^{1}H$-$\{^{11}B$(off-resonance)$\}$ spectrum is subtracted from a $^{1}H$-$\{^{11}B$(on-resonance)$\}$ spectrum in order to eliminate $^{1}H$ lines not coupled to the boron nuclei of interest. 128-MHz $^{11}B$, $^{11}B$-$\{^{1}H$(broad-band noise)$\}$ and two-dimensional [$^{11}B$–$^{11}B$]-COSY experiments (Figures 2, 4, and 5) were done on a Bruker AM-400 instrument. The two-dimensional [$^{11}B$–$^{11}B$]-COSY experiments were acquired with a 90° pulse [compounds (**2**)—(**4**)] and also [compounds (**2**) and (**3**)] a 45° pulse in order to reduce the intensity of the ($F_1 = F_2$) diagonal and hence observe, unambiguously, correlations between closely grouped resonances. The parameters were chosen such that the acquisition times in the $t_2$ and $t_1$ dimensions were *ca.* 31 and 8 ms [(**2**) and (**3**)] or *ca.* 18 and 9 ms [(**4**)], respectively. A total of 128 increments with increment sizes of 60 [(**2**) and (**3**)] or 72 μs [(**4**)] were collected in all cases. The total acquisition times varied from *ca.* 30 min [(**2**) and (**3**)] to *ca.* 8 h [(**4**)], uninterrupted $\{^{1}H$(broad-band noise)$\}$ decoupling being applied throughout. The data were zero-filled in the $t_1$ dimension such as to achieve identical digitization in both dimensions [*i.e.* × 4 for (**2**) and (**3**) (digital resolution 32 Hz), and × 2 for (**4**) (digital resolution 56 Hz)] and multiplied by a sine-bell or sine-bell squared function (to reduce the tailing of the resonances) prior to Fourier transformation. The frequency domain matrices were symmetrized along their ($F_1 = F_2$) diagonal. The COSY experiments were done on samples held at elevated temperatures (generally *ca.* 363 K) so as to reduce the $^{11}B$ quadrupolar relaxation rates thus decreasing the natural linewidths and enabling correlations to be more readily observed for smaller couplings.[23,26] Chemical shifts $\delta(^{1}H)$, $\delta(^{31}P)$, and $\delta(^{11}B)$ are given in p.p.m. to high frequency (low field) of Ξ 100 (nominally $SiMe_4$), Ξ 40.480 730 (nominally 85% $H_3PO_4$), and Ξ 32.083 971 MHz [nominally $BF_3(OEt_2)$ in $CDCl_3$ solution][23] respectively.

## Acknowledgements

We thank the S.E.R.C. for support and Dr. D. Reed (Edinburgh University) for some services in $^{1}H$-$\{^{11}B\}$ n.m.r. spectroscopy in the initial stages of the work.

## References

1 Part 1, X. L. R. Fontaine, H. Fowkes, N. N. Greenwood, J. D. Kennedy, and M. Thornton-Pett, *J. Chem. Soc., Dalton Trans.*, 1986, 547.
2 H. Fowkes, results presented to 'The Fourth National Meeting of British Inorganic Boron Chemists,' INTRABORON-4, Durham, September, 1984.
3 M. Thornton-Pett, results presented to 'The 1985 Meeting of the British Crystallographic Association,' Bristol, 25—27th March, 1985.
4 N. N. Greenwood, *Nova Acta Leopold.*, 1985, **59**, 291.
5 X. L. R. Fontaine, H. Fowkes, N. N. Greenwood, J. D. Kennedy, and M. Thornton-Pett, *J. Chem. Soc., Chem. Commun.*, 1985, 1165.
6 X. L. R. Fontaine, H. Fowkes, N. N. Greenwood, J. D. Kennedy, and M. Thornton-Pett, *J. Chem. Soc., Chem. Commun.*, 1985, 1722.
7 H. Fowkes, N. N. Greenwood, J. D. Kennedy, and M. Thornton-Pett, *J. Chem. Soc., Dalton Trans.*, 1985, 517.
8 X. L. R. Fontaine, N. N. Greenwood, J. D. Kennedy, P. MacKinnon, and M. Thornton-Pett, *J. Chem. Soc., Chem. Commun.*, 1986, 1111 and refs. therein.
9 J. D. Kennedy, *Prog. Inorg. Chem.*, 1984, **32**, 579; 1986, **34**, 211 and refs. therein.
10 (*a*) M. Bown, unpublished work, University of Leeds, 1986; (*b*) M. A. Beckett, J. E. Crook, N. N. Greenwood, and J. D. Kennedy, *J. Chem. Soc., Dalton Trans.*, 1986, 1879.
11 N. N. Greenwood, J. D. Kennedy, M. Thornton-Pett, and J. D. Woollins, *J. Chem. Soc., Dalton Trans.*, 1985, 2397.
12 See, for example, S. G. Shore, in 'Boron Hydride Chemistry,' ed. E. L. Muetterties, Academic Press, London and New York, 1975, pp. 119—120 and refs. therein.
13 J. Bould, Ph.D. Thesis, University of Leeds, 1983.
14 T. L. Venable and R. N. Grimes, *Inorg. Chem.*, 1982, **21**, 887; T. L. Venable, E. Sinn, and R. N. Grimes, *ibid.*, p. 895.
15 T. L. Venable, E. Sinn, and R. N. Grimes, *J. Chem. Soc., Dalton Trans.*, 1984, 2275.
16 See, for example, J. J. Briguglio and L. G. Sneddon, *Organometallics*, 1986, **5**, 327 and refs. therein.
17 I. J. Colquhoun and W. McFarlane, results presented to 'The First and Third National Meetings of British Inorganic Boron Chemists,' INTRABORON-1, Strathclyde, May 1980, and INTRABORON-3, Leeds, September 1982.
18 T. L. Venable, W. C. Hutton, and R. N. Grimes, *J. Am. Chem. Soc.*, 1982, **104**, 4716; 1984, **106**, 29.
19 D. Reed, *J. Chem. Res. S*, 1984, 198.
20 J. D. Kennedy and N. N. Greenwood, *Inorg. Chim. Acta*, 1980, **38**, 93.
21 S. K. Boocock, N. N. Greenwood, M. J. Hails, J. D. Kennedy, and W. S. McDonald, *J. Chem. Soc., Dalton Trans.*, 1981, 1415.
22 See, for example, D. F. Gaines, C. K. Nelson, J. C. Kunz, J. H. Morris, and D. Reed, *Inorg. Chem.*, 1984, **23**, 3252.
23 J. D. Kennedy, 'Multinuclear N.M.R.,' ed. J. Mason, Plenum, London and New York, ch. 8, in the press and refs. therein.
24 M. A. Beckett, N. N. Greenwood, J. D. Kennedy, and M. Thornton-Pett, *J. Chem. Soc., Dalton Trans.*, 1986, 795.
25 R. F. Sprecher, B. E. Aufderheide, G. W. Luther, and J. C. Carter, *J. Am. Chem. Soc.*, 1974, **96**, 4404.
26 X. L. R. Fontaine and J. D. Kennedy, *J. Chem. Soc., Chem. Commun.*, 1986, 779.
27 R. N. Leyden and M. F. Hawthorne, *J. Chem. Soc., Chem. Commun.*, 1975, 310.
28 R. N. Leyden, B. P. Sullivan, R. T. Baker, and M. F. Hawthorne, *J. Am. Chem. Soc.*, 1978, **100**, 3758.
29 N. N. Greenwood, M. J. Hails, J. D. Kennedy, and W. S. McDonald, *J. Chem. Soc., Dalton Trans.*, 1985, 983.
30 J. Bould, N. N. Greenwood, J. D. Kennedy, and W. S. McDonald, *J. Chem. Soc., Chem. Commun.*, 1982, 465.
31 R. P. Micciche, J. J. Briguglio, and L. G. Sneddon, *Inorg. Chem.*, 1984, **23**, 3992.
32 J. E. Crook, M. Elrington, N. N. Greenwood, J. D. Kennedy, M. Thornton-Pett, and J. D. Woollins, *J. Chem. Soc., Dalton Trans.*, 1985, 2407.
33 M. Bown, N. N. Greenwood, and J. D. Kennedy, *J. Organomet. Chem.*, 1986, **309**, C67.
34 R. N. Grimes, in 'Comprehensive Organometallic Chemistry,' eds. G. Wilkinson, F. G. A. Stone, and E. Abel, Pergamon, Oxford, 1982, Part I, ch. 5.5, pp. 459—542 and refs. therein.
35 A. I. Yanovskii, *Russ. Chem. Rev.* (*Engl. Transl.*), 1985, **54**, 515 and refs. therein.
36 J. E. Crook, N. N. Greenwood, J. D. Kennedy, and W. S. McDonald, *J. Chem. Soc., Chem. Commun.*, 1983, 83.
37 N. W. Alcock, J. G. Taylor, and M. G. H. Wallbridge, *J. Chem. Soc., Chem. Commun.*, 1982, 383.
38 L. Barton, in 'Topics in Current Chemistry 100: New Trends in Chemistry,' ed. F. L. Boschke, Springer, Berlin, 1983, pp. 3—204.
39 J. Kroner and B. Wrackmeyer, *J. Chem. Soc., Faraday Trans. 2*, 1976, 2283.
40 T. Onak, J. B. Leach, S. Anderson, and M. F. Frisch, *J. Magn. Reson.*, 1976, **23**, 237.
41 W. Jarvis, Z. J. Abdon, and T. Onak, *Polyhedron*, 1983, **2**, 1067.
42 Y. M. McInnes, unpublished work, University of Leeds, 1984—1986.
43 J. Bould, N. N. Greenwood, and J. D. Kennedy, *J. Chem. Soc., Dalton Trans.*, 1984, 2477.
44 M. Bown, M. A. Beckett, X. L. R. Fontaine, N. N. Greenwood, J. D. Kennedy, and M. Thornton-Pett, unpublished work.
45 G. B. Jacobsen, D. G. Meina, J. H. Morris, C. Thompson, S. J. Andrews, D. Reed, A. J. Welch, and D. F. Gaines, *J. Chem. Soc., Dalton Trans.*, 1985, 1645.
46 A. B. Burg, *J. Am. Chem. Soc.*, 1968, **90**, 1407.

47 See, for example, D. F. Gaines, *Acc. Chem. Res.*, 1973, **6**, 416; in, 'Boron Chemistry–4,' eds. R. W. Parry and G. Kodama, Pergamon, 1980, pp. 95—107 and refs. therein.
48 J. W. Lott, D. F. Gaines, H. Shenhav, and R. Schaeffer, *J. Am. Chem. Soc.*, 1973, **95**, 3042.
49 D. F. Gaines, J. W. Lott, and J. C. Calabrese, *J. Chem. Soc., Chem. Commun.*, 1973, 295; *Inorg. Chem.*, 1974, **13**, 2419.
50 J. W. Lott and D. F. Gaines, *Inorg. Chem.*, 1974, **13**, 2261.
51 M. A. Beckett, N. N. Greenwood, J. D. Kennedy, and M. Thornton-Pett, *J. Chem. Soc., Dalton Trans.*, 1985, 1119.
52 N. N. Greenwood, J. D. Kennedy, I. Macpherson, and M. Thornton-Pett, *Z. Anorg. Allg. Chem.*, 1986, **540/541**, 45.
53 J. Bould, J. D. Kennedy, and N. N. Greenwood, *J. Organomet. Chem.*, 1983, **249**, 11.
54 J. Bould, J. E. Crook, N. N. Greenwood, and J. D. Kennedy, unpublished work.
55 A. Modinos and P. Woodward, *J. Chem. Soc., Dalton Trans.*, 1981, 1415.
56 N. Walker and D. Stuart, *Acta Crystallogr., Sect. A*, 1983, **39**, 158.
57 G. M. Sheldrick, SHELX 76, Program System for *X*-Ray Structure Determination, University of Cambridge, 1976.
58 S. K. Boocock, J. Bould, N. N. Greenwood, J. D. Kennedy, and W. S. McDonald, *J. Chem. Soc., Dalton Trans.*, 1982, 713.
59 T. C. Gibb and J. D. Kennedy, *J. Chem. Soc., Faraday Trans. 2*, 1982, 5251.
60 J. D. Kennedy and B. Wrackmeyer, *J. Magn. Reson.*, 1980, **38**, 529.
61 J. D. Kennedy and J. Staves, *Z. Naturforsch., Teil B*, 1979, **34**, 808.

*Received* 1*st July* 1986; *Paper* 6/1325